Title

Caveolin-3 Overexpression Attenuates Cardiac Hypertrophy via Inhibition of T-type Ca2+ Current Modulated by Protein Kinase Cα in Cardiomyocytes*

Journal

Journal of Biological Chemistry, 290(36)

ISSN

0021-9258

Authors

Markandeya, Yogananda S

Phelan, Laura J

Woon, Marites T

et al.

Publication Date

2015-09-01

DOI

10.1074/jbc.m115.674945

THE JOURNAL OF BIOLOGICAL CHEMISTRY VOL. 290, NO. 36, pp. 22085–22100, September 4, 2015
Published in the U.S.A.

Caveolin-3 Overexpression Attenuates Cardiac Hypertrophy via Inhibition of T-type Ca^{2+} Current Modulated by Protein Kinase Cα in Cardiomyocytes*

Received for publication, June 25, 2015 Published, JBC Papers in Press, July 13, 2015, DOI 10.1074/jbc.M115.674945

Yogananda S. Markandeya[‡], Laura J. Phelan[‡], Marites T. Woon[‡], Alexis M. Keefe[‡], Courtney R. Reynolds[‡], Benjamin K. August[‡], Timothy A. Hacker[‡], David M. Roth[§¶], Hemal H. Patel[§¶], and Ravi C. Balijepalli[‡1]

From the [‡]Cellular and Molecular Arrhythmia Research Program, Department of Medicine, University of Wisconsin, Madison, Wisconsin 53706, the [§]Veterans Affairs San Diego Healthcare Systems, San Diego, California 92161, and the [¶]Department of Anesthesiology, University of California at San Diego, La Jolla, California 92161

Background: Ventricular remodeling altered caveolin-3 expression, and Ca^{2+} signaling is associated with cardiac hypertrophy.
Results: Cardiomyocyte-specific caveolin-3 overexpression prevented cardiac hypertrophy by inhibiting the T-type Ca^{2+} current and hyperactivation of calcineurin-dependent nuclear factor of activated T-cell signaling.
Conclusion: Caveolin-3 expression is essential for protective Ca^{2+} signaling in pathological cardiac hypertrophy.
Significance: Caveolin-3 overexpression in heart may be used as a therapeutic strategy for treatment of many cardiovascular diseases.

Pathological cardiac hypertrophy is characterized by subcellular remodeling of the ventricular myocyte with a reduction in the scaffolding protein caveolin-3 (Cav-3), altered Ca^{2+} cycling, increased protein kinase C expression, and hyperactivation of calcineurin/nuclear factor of activated T cell (NFAT) signaling. However, the precise role of Cav-3 in the regulation of local Ca^{2+} signaling in pathological cardiac hypertrophy is unclear. We used cardiac-specific Cav-3-overexpressing mice and *in vivo* and *in vitro* cardiac hypertrophy models to determine the essential requirement for Cav-3 expression in protection against pharmacologically and pressure overload-induced cardiac hypertrophy. Transverse aortic constriction and angiotensin-II (Ang-II) infusion in wild type (WT) mice resulted in cardiac hypertrophy characterized by significant reduction in fractional shortening, ejection fraction, and a reduced expression of Cav-3. In addition, association of PKCα and angiotensin-II receptor, type 1, with Cav-3 was disrupted in the hypertrophic ventricular myocytes. Whole cell patch clamp analysis demonstrated increased expression of T-type Ca^{2+} current ($I_{Ca,T}$) in hypertrophic ventricular myocytes. In contrast, the Cav-3-overexpressing mice demonstrated protection from transverse aortic constriction or Ang-II-induced pathological hypertrophy with inhibition of $I_{Ca,T}$ and intact Cav-3-associated macromolecular signaling complexes. siRNA-mediated knockdown of Cav-3 in the neonatal cardiomyocytes resulted in enhanced Ang-II stimulation of $I_{Ca,T}$ mediated by PKCα, which caused nuclear translocation of NFAT. Overexpression of Cav-3 in neonatal myocytes prevented a PKCα-mediated increase in $I_{Ca,T}$ and nuclear translocation of NFAT. In conclusion, we show that stable Cav-3 expression is essential for protecting the signaling mechanisms in pharmacologically and pressure overload-induced cardiac hypertrophy.

Cardiac hypertrophy is a major predictor of many cardiovascular diseases, including arrhythmias, sudden death, and heart failure. Cardiac hypertrophy is an adaptive response of the heart during stress to preserve contractility and cardiac function. However, continued cardiac stress through either pressure or volume overload or neurohormonal stress leads to pathological hypertrophy and heart failure (1, 2), during which an alteration in cardiac myocyte Ca^{2+} handling is commonly observed (3–5). It is well established that an increase in cytosolic Ca^{2+} is responsible for activating calcineurin (Cn)[2] and nuclear factor of activated T-cell (NFAT) signaling leading to the expression of genes involved in pathological cardiac hypertrophy. With the progression of cardiac hypertrophy, a structural remodeling of the ventricular myocytes results in T-tubule disruption at advanced heart failure (6). With myocyte remodeling during cardiac hypertrophy and heart failure (7, 8), it is likely that the micro-architecture of the sarcolemma and T-tubules, which are major determinants of the local control of Ca^{2+} in the heart, is altered.

* This work was supported, in whole or in part, by National Institutes of Health Grants HL105713 (to R. C. B.), HL091071 (to H. H. P.), HL107200 (to H. H. P.), HL066941 (to D. M. R.), and HL115933 (to D. M. R.) from NHLBI. This work was also supported by the United States Department of Veterans Affairs (Washington D. C.) Grants BX001963 (to H. H. P.) and BX000783 (to D. M. R.) and American Heart Association Grant-in-aid 11GRNT7610094 (to R. C. B.). The authors declare that they have no conflicts of interest with the contents of this article.

[1] To whom correspondence should be addressed: Dept. of Medicine, University of Wisconsin School of Medicine and Public Health, 1111 Highland Ave., Rm. 8405 WIMR-II, Madison, WI 53706. Tel.: 608-263-4066; Fax: 608-263-1144; E-mail: rcb@medicine.wisc.edu.

[2] The abbreviations used are: Cn, calcineurin; Cav-3, caveolin-3; TTCC, T-type calcium channel; Ang-II, angiotensin II; $I_{Ca,T}$, T-type calcium channel current; $I_{Ca,L}$, L-type calcium channel current; NFAT, nuclear factor of activated T-cells; OE, overexpression; NMVM, neonatal mouse ventricular myocytes; TAC, transthoracic aortic constriction; pF, picofarad; TRPC, transient receptor potential; co-IP, co-immunoprecipitated; HW/BW, heart weight to body weight; AT1-R, angiotensin receptor type 1; eGFP, enhanced GFP; qPCR, quantitative PCR; AT1, angiotensin II receptor, type 1; TAC, transverse aortic constriction; LTCC, L-type Ca^{2+} channel.

Caveolae are specialized microdomains in the sarcolemmal membrane of ventricular myocytes that serve to integrate sympathetic and parasympathetic inputs to the heart to precisely regulate cardiac function. Caveolae contain a variety of signaling proteins such as G-protein-coupled receptors, kinases, phosphatases, and ion channels, including the voltage-gated L-type and the T-type Ca^{2+} channels and other calcium cycling proteins (9–11). Caveolin-3 (Cav-3) is a muscle-specific scaffolding protein integral to caveolae in the cardiomyocyte and plays a significant role in the physiology of the heart (12). Reduced expression of Cav-3 and caveolae in cardiomyocytes is reported in cardiac diseases, including myocardial infarction and heart failure (13). In contrast, we have shown that overexpression of Cav-3 prevents ischemic injury (14) and cardiac hypertrophy (15). However, the precise role of Cav-3 in the regulation of local Ca^{2+} signaling and regulation of pathophysiology in cardiac hypertrophy is unclear.

In this study, we determined whether a loss of Cav-3 expression during pressure overload and angiotensin-II (Ang-II) treatment contributes to altered Ca^{2+}-induced Cn-NFAT signaling and the development of pathological cardiac hypertrophy. We demonstrated that a loss of Cav-3 expression after pressure overload or Ang-II treatment results in the disruption of caveola-associated macromolecular signaling proteins, increased stimulation of T-type Ca^{2+} channels (TTCC) current ($I_{Ca,\,T}$) mediated by PKCα, and the activation of Cn-NFAT signaling in cardiomyocytes. Additionally, Cav-3 overexpression in cardiomyocytes inhibits basal and Ang-II-stimulated $I_{Ca,\,T}$ that is modulated by PKCα and the activation of Cn-NFAT signaling. Using mice with cardiac-specific overexpression Cav-3 (Cav-3 OE) (14), generated using the α-myosin heavy chain promoter system, we demonstrated that development of pressure overload-induced pathological cardiac hypertrophy *in vivo* is prevented.

Materials and Methods

Transverse Aortic Constriction (TAC) induced Pressure Overload Hypertrophy—TAC was performed in 12–16-week-old male mice to induce pressure overload as described earlier (16). Briefly, the mice were anesthetized with 2% isofluorane inhalation, and insertion was made to expose the aorta. A 27-gauge needle was placed on top of the aorta and ligated using 7-0 silk sutures, following which the needle was removed to produce refined stenosis of the vessel. The muscle cavity and skin were sutured, and the wound was closed with wound clip. Mice of the same genetic background received a sham operation in which a silk suture band was placed around the aorta but not ligated and was subsequently removed.

Ang-II Infusion Induced Cardiac Hypertrophy—Ang-II or saline was infused for 28 days using mini osmotic pumps (model 2002, ALZET Osmotic Pumps, Cupertino, CA). Osmotic pumps primed at constant rate of 0.5 μg/h, filled with 5 mg/ml Ang-II (Sigma) or isotonic saline, were inserted subcutaneously above the scapula under sterile conditions in anesthetized mice. For *in vitro* Ang-II-induced cardiac hypertrophy, NMVM were isolated from 1- to 2-day-old pups and grown in culture treated with Ang-II (10μmol/liter) for 48 h.

Echocardiography Analysis—Noninvasive transthoracic echocardiography was performed using Visual Sonics Vevo 770 ultrasonograph. ECG was monitored continuously in anesthetized mice (1.5% isoflurane) maintained on a heated platform. After 4 weeks of saline or Ang-II infusion and sham or TAC surgery in mice, left ventricular wall thickness, chamber dimensions, and contractility were evaluated. The pressure gradients across the aortic constriction were measured to ensure similar pressure overload in the TAC mice.

Transmission Electron Microscopy—Rapidly excised mouse hearts were initially perfused with Tyrode's solution (10 ml) in a Langendorff perfusion system followed by fixative (2.5% glutaraldehyde, 2.0% paraformaldehyde) in 0.1 mol/liter cacodylate buffer for 30 min. The left ventricle was dissected out, cut into 2 × 2-mm blocks, immersed in the same fixative, and left overnight at 4 °C. The samples were rinsed in the same buffer, postfixed in 1% osmium tetroxide, dehydrated in a graded ethanol series, rinsed in propylene oxide, and embedded in Epon 812 substitute. After resin polymerization, the samples were then sliced into 70-nm sections with a Leica EM UC6 ultramicrotome and placed on 200 mesh transmission electron microscopy grids. The samples were post-stained in 8% uranyl acetate in 50% EtOH and Reynold's lead citrate, viewed on a Philips CM120 transmission electron microscope, and documented with a SIS MegaView III digital camera. A relative number of caveolae distributed in the myocyte sarcolemmal membranes was estimated by obtaining about 250 images from three preparations of WT or TAC samples. A threshold size for individual caveolae was set between 40 and 100 nm. The number of caveolae was counted as per unit length (μm) of myocyte sarcolemmal membranes using ImageJ software from a series of random EM micrographs. To confirm caveola vesicles from other regions, immunogold labeling using anti-Cav-3 antibody was performed. Data were analyzed by plotting frequency histograms of the number of caveolae per μm of sarcolemma for each observation.

Isolation of Mouse Ventricular Myocytes—Neonatal or adult mouse ventricular myocytes were enzymatically isolated as described previously (11). Rod-shaped myocytes with clear striations were randomly selected for electrophysiology studies. The neonatal myocytes were transfected by the electroporation method (11) by a Nucleofector device (Lonza, USA) using Ingenio electroporation reagent (catalog no. MIR 50115) from Mirus BioSciences, and cells were used for experiments 72–96 h after transfection.

siRNA-mediated Cav-3 Knockdown and shRNA-mediated PKCα Knockdown—siRNA-mediated knockdown of Cav-3 in isolated neonatal mouse cardiomyocytes was archived by transfecting three pairs of pre-validated Cav-3-specific siRNAs (10 nmol/liter) as described earlier (11, 18). For shRNA-mediated knockdown of PKCα, the neonatal myocytes were transfected with 1 μg of plasmid containing an shRNA sequence specific for the PKCα isoform (5′-GAACAACAAGGAAUGACUU-3′ (19), a kind gift from Dr. Scott Kaufmann (Mayo Clinic, Rochester, MN).

Quantitative Real Time PCR Analysis—MIQE guidelines were followed in designing qPCR experiments. Total RNA isolated from SHAM, TAC, saline, and Ang-II treated mouse left

ventricles using the GenElute Mammalian Total RNA Miniprep kit (Sigma). RNA quantity and quality were determined with UV spectrophotometry. First strand cDNA synthesis was performed with 1 μg of total RNA using iScript reverse transcription supermix for RT-qPCR (Bio-Rad). The levels of cDNA were analyzed by quantitative real time PCR using TaqMan gene expression master mix (Applied Biosystems). Probes and primers were designed for multiplex analysis (Integrated DNA Technologies). Primers and probes designed for analysis of the genes of interest are provided in Table 1. RT-qPCR was performed on CFX96^{TM} real time systems (Bio Rad). For quantification of mRNA levels, the normalized cycle values were obtained by the subtraction of corresponding GAPDH (ΔC_T), and data are presented as fold change (for TAC or Ang-II treatment) with respect to expression in SHAM or saline-treated samples ($\Delta\Delta C_T$).

Preparation of Caveolin-enriched Fractions—Caveolin-enriched membrane fractions from mouse ventricular myocytes from WT or Cav-3 OE following TAC or sham treatment were prepared by using a previously described method (18). Briefly, freshly isolated adult mouse myocytes (10×10^6 cells) were suspended in 2 ml of ice-cold 0.5 mol/liter sodium carbonate (pH 11.0) and homogenized sequentially by using a loose-fitting Dounce homogenizer (10 strokes), a Polytron tissue grinder (three 10-s bursts; Kinematica, Brinkmann Instruments, Westbury, NY), and a sonicator (three 20-s bursts; Branson Sonifier 250, Branson Ultrasonic, Danbury, CT). The homogenate was adjusted to 45% sucrose in MBS (25 mmol/liter Mes (pH 6.5), 0.15 mol/liter NaCl) and placed at the bottom of an ultracentrifuge tube. A 5–35% discontinuous sucrose gradient (in MBS containing 250 mmol/liter sodium carbonate) was formed and centrifuged at 39,000 rpm for 16–20 h in an SW41 rotor (Beckman Instruments, Palo Alto, CA). From the bottom of each gradient, 1-ml gradient fractions were collected to yield a total of 12 fractions. Protein concentrations determined by the Lowry assay (Bio-Rad) confirmed that total protein distribution was weighted toward heavier sucrose density gradient fractions (F7 through F11). A light-scattering band confined to fractions 4–6 typically corresponds to caveola-enriched fractions. Proteins from different fractions were precipitated using 0.1% w/v deoxycholic acid in 100% w/v trichloroacetic acid and then each fraction sample was solubilized into an equal volume (40 μl) of sample buffer for SDS-PAGE and Western blot analysis.

Antibodies—$Ca_v3.1$ and $Ca_v3.2$ were from Alomone Labs (Jerusalem, Israel); Cav-3, PKCα, angiotensin receptor type 1, nitric-oxide synthase 3 (NOS-3) were from BD Biosciences, and β_1-adrenergic receptor, PKCβ1, and NFATc3 were from Santa Cruz Biotechnology, Inc.

Co-immunoprecipitation and Western Blot Analysis—Isolated adult mouse myocytes (~2 mg of protein) were rinsed with ice-cold 25 mmol/liter Tris-HCl (pH 7.4), 150 mmol/liter NaCl (TBS), and lysed in ice-cold solubilization buffer containing 25 mmol/liter Tris-HCl (pH 7.4), 150 mmol/liter NaCl, 60 mmol/liter *n*-octyl D-glucoside, 1% Triton X-100, 2 mmol/liter phenylmethylsulfonyl fluoride, 5 μg/ml aprotinin, 5 μg/ml benzamidine, 5 μg/ml leupeptin, and 5 μmol/liter pepstatin A. The lysate was centrifuged at 10,000 $\times$ *g* for 10 min to remove insol-

TABLE 1
qRT-PCR primers and probes
Ref indicates reference.

Gene	Accession no.	Amplicon size	Forward Ref start	Forward Ref end	Forward T_m	Forward oligonucleotide sequence	Probe Ref start	Probe Ref end	Probe T_m	Probe oligonucleotide sequence	Reverse Ref Start	Reverse Ref End	Rev TM	Reverse oligonucleotide sequence
ANP	NM_008725	108	119	137	61.8	CTTCCTCGTCTTGGCCTTT	162	185	68.0	AATCCTGTGTACAGTGCGGTGTCC	208	226	62.1	AGGTGGTCTAGCAGGTTCT
BNP	NM_008726	111	490	509	62.0	GCACAAGATAGACCGGATCG	525	548	68.4	ACAACTTCAGTGCGTTACAGCCCA	582	600	62.0	CCCAGGCAGAGTCAGAAAC
Cav1	NM_007616	105	107	127	62.6	CGAGGGACATCTCTACACTGT	134	156	68.0	CCGGGAACAGGGCAACATCTACA	191	211	62.5	GCGTCATACACTTGCTTCTCA
Cav3	NM_007617	106	397	414	61.9	GCGACCCCAAGAACATCA	425	455	68.5	CGCAATCACGTCTTCAAAATCTACCTTCACA	483	502	61.7	AAGCTCACCTTCCATACACC
$Ca_v3.1$	NM_009783	124	4446	4467	61.7	CTCAACTGTATCACCATCGCTA	4498	4521	67.4	CTGAACGCATCTTCCTGACCCTCT	4549	4569	62.7	CCTTCACTGTCATTTCAGCCA
$Ca_v3.2$	NM_021415	108	2725	2745	62.0	CAGCCATCCTCGTCAATACTCC	2773	2795	67.9	AGCCTGATGAGCTGACTAACGCG	2813	2832	62.1	CAAACATGCTGGTGAACACG
$Ca_v1.2$	NM_009781	114	1293	1312	61.5	GCATCACCAACTTCGACAAC	1360	1383	67.3	ATCCAGTACAGCACGTCTGTCCAG	1387	1406	62.5	ACTCATAGCCCATAGCGTCT
SERCA2a	NM_001163336	131	2462	2482	61.8	GTTCATCCGCTACCTCATCTC	2488	2511	68.3	AGATGCAGACAACCTCGCCAACAT	2572	2592	61.7	GTAAGCCATCTGTTACCAGGT
Gapdh	NM_008084	118	886	905	62.2	TTGTCTCCTGCGACTTCAAC	911	934	67.9	CTCCCACTCTTCCACCTTCGATGC	981	1003	61.8	TAGCCGTATTCATTGTCATACCA

uble debris, and the soluble supernatant was precleared by using protein G Dynabeads (Invitrogen), followed by incubation for 4 h at 4 °C with anti-Cav-3 (2 μg) antibodies or control IgG in a total of 450 μl. 50 μl of a 1:1 slurry of protein G Dynabeads was added to the sample and further incubated for 1 h at 4 °C. Beads were washed four times with solubilization buffer on a magnetic stand, and bound proteins were eluted with SDS-PAGE sample buffer by boiling for 5 min. Immune complexes were analyzed by SDS-PAGE (4–15% gradient gels, Bio-Rad) and Western blot by probing with antibodies to Cav-3, PKCα, angiotensin receptor type 1, NOS-3, and β_1AR.

Electrophysiology—Electrophysiological experiments were carried out using the whole cell patch clamp technique using Axopatch 200B amplifier (Axon Instruments, Foster City, CA) with pClamp version 10.2 software. The patch pipettes were pulled from thin-walled borosilicate glass capillaries (World Precision Instruments, Inc., Sarasota, FL) on Sutter P-87 micropipette puller (Sutter Instrument Co.) and polished using microforge MF900 (Narishige). All the experiments were carried out at room temperature with pipette resistance of 1.5–2.5 megohms. Recordings were made from the freshly isolated healthy rod-shaped ventricular myocytes. The bath solution to measure T-type Ca^{2+} channel currents from adult cardiomyocytes consisted of (in mmol/liter) 140 TEA-Cl, 1 $MgCl_2$, 1.8 $CaCl_2$, 10 glucose, and 10 HEPES (pH 7.4), tetradotoxin 20 μmol/liter. For neonatal cardiomyocytes, bath buffer consisted of (in mmol/liter) 145 TEA-Cl, 5 $CaCl_2$, 1 $MgCl_2$, 5 CsCl, 1,4-aminopyridine, 0.01 tetradotoxin, 10 HEPES, 5 D-glucose (pH 7.4), adjusted with TEA-OH. The internal pipette solution consisted of (in mmol/liter) 114 CsCl, 10 EGTA, 10 HEPES, 5 MgATP (pH 7.2) adjusted using CsOH. T- and L-type calcium currents were measured using a dual pulse protocol as described earlier by us (11). Myocytes were held at a holding potential of −90 mV, and a 10-mV step depolarization was applied up to +60 mV for 200 ms ($I_{Ca,\ total}$), followed by a brief holding potential of −50 mV, and a further 10-mV step depolarization was applied up to +70 mV for 200 ms ($I_{Ca,\ L}$). First pulse represents the total current ($I_{Ca,\ total}$), and the second pulse represents the L-type current ($I_{Ca,\ L}$). T- type calcium current ($I_{Ca,\ T}$) was obtained by subtracting $I_{Ca,\ L}$ traces from $I_{Ca,\ total}$ and indicated as $I_{Ca,\ difference}$ ($I_{Ca,\ diff}$). When this $I_{Ca,\ T}$ is absent (absence of peak I_{Ca} at −30 mV) in the cells, the two *I-V* curves generated from holding potentials of −90 and −50 mV will overlap but may also exhibit a $I_{Ca,\ diff}$ at, or membrane potentials positive to −10 mV. A small difference in the currents at potentials positive to −10 mV was not due to the presence of $I_{Ca,\ T}$ but could be due to partial voltage-dependent inactivation of $I_{Ca,\ L}$ recorded with a holding potential of −50 mV. The current traces were corrected for linear capacitance and leak using −P/4 subtraction. The data were filtered at 5 kHz and digitized at 50 kHz and were analyzed using Microcal Origin software (Origin Lab Corp., Northampton, MA). The data were analyzed using OriginPro.9.0.0 (OriginLab Corp.).

Statistics—Statistical significance was analyzed with Student's paired *t* test. Average data are reported as mean ± S.E.

Results

Cav-3 and Caveola Expression Is Altered in Ventricular Myocytes in TAC or Ang-II Infusion-induced Cardiac Hypertrophy—Previous studies have indicated that the level of Cav-3 expression and the density of caveolae can change in various models of cardiac disease, including cardiac hypertrophy and heart failure (13, 20). We investigated for changes in the expression of Cav-3 in mouse models of pressure overload-induced cardiac hypertrophy. 12–16-Week-old C57BL6 mice were chronically treated with Ang-II via continuous infusion (via mini osmotic pumps; see under "Materials and Methods") or TAC surgery. Cardiac function was measured by echocardiography before TAC, sham, or Ang-II or saline treatment and then after 4 weeks of treatment. Four weeks of TAC or Ang-II treatment resulted in the development of pathological cardiac hypertrophy as evidenced by significant changes in HW/BW, and reduced fractional shortening and ejection fraction in the WT mice compared with sham or saline-treated mice (Fig. 1, *A–C*). The RNA isolated from left ventricular myocytes showed a significant increase in atrial natriuretic peptide, B-type natriuretic peptide expression, and a significant reduction in the expression for Cav-3 and SERCA2a levels in TAC- and Ang-II-treated mice compared with sham or saline-treated mice (Fig. 2, *A* and *B*). The mRNA levels for Cav-1 were unchanged between the groups. We then estimated the expression of Cav-3 protein by semi-quantitative Western blot analysis in mouse ventricular myocytes. Cav-3 expression levels (Fig. 1, *D* and *E*) were significantly reduced (~50%) after TAC- or Ang-II-induced cardiac hypertrophy when compared with control hearts (sham or saline infusion). We then performed transmission electron microscopy analysis on the left ventricle tissue sections after 4 weeks of TAC or sham treatment. As shown in the representative electron micrograph (Fig. 1*F*), after 4 weeks of TAC, the number of caveolae was reduced significantly (64%) in the left ventricular myocytes compared with the sham mice (Fig. 1*G*).

$I_{Ca,\ T}$ Is Up-regulated in Left Ventricular Myocytes in Cardiac Hypertrophy—Previous studies have shown that $I_{Ca,\ T}$ is expressed only during cardiac development and is undetectable in adult ventricular myocytes (21, 22). However, $I_{Ca,\ T}$ was shown to be re-expressed in ventricular myocytes in diseased hearts, including pressure overload-induced cardiac hypertrophy (11, 23, 24) in cardiomyopathic hamster (25), and in post-infarction remodeled rat left ventricle (26). We measured the expression levels for the TTCC subunit isoforms, $Ca_v3.1$ and $Ca_v3.2$, in the ventricles by qPCR analysis. We noticed an increased mRNA expression for $Ca_v3.1$ and $Ca_v3.2$ subunits in the left ventricles from TAC- or Ang-II-treated mice compared with vehicle- or sham-treated mice, respectively (Fig. 2, *A* and *B*). The mRNA levels for $Ca_v3.2$ appeared to be significantly higher ($p < 0.05$) in the TAC ventricle compared with sham (Fig. 2*A*). In contrast, the mRNA levels for the $Ca_v1.2$ subunit of the LTCC did not change after TAC or Ang-II treatment compared with controls. We then investigated whether the $I_{Ca,\ T}$ was detectable in the adult left ventricular myocytes after TAC or Ang-II infusion. $I_{Ca,\ T}$ and L-type Ca^{2+} channel current ($I_{Ca,\ L}$) were measured using the whole cell patch clamp technique by applying a dual pulse protocol described previously by

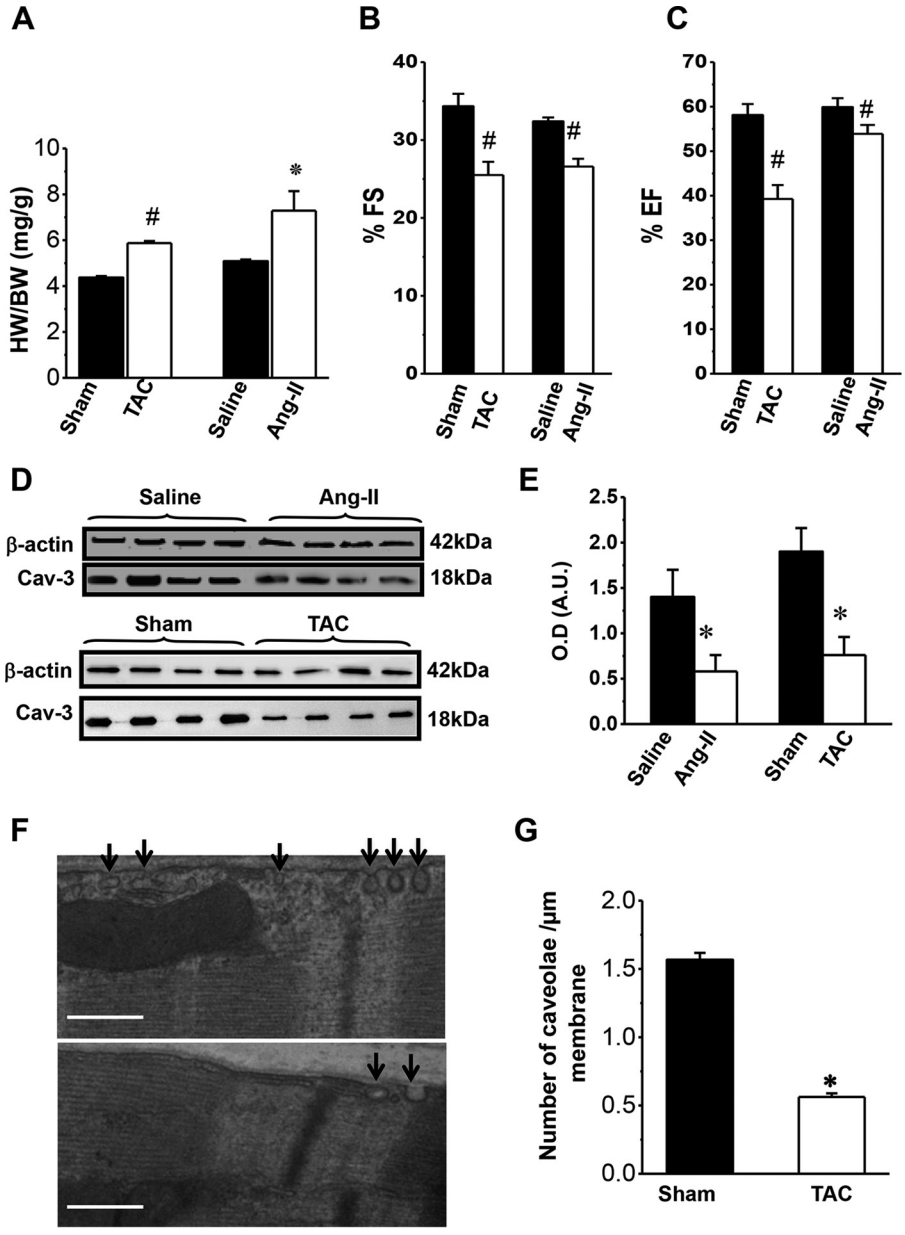

FIGURE 1. **Reduced Cav-3 and caveola expression levels in ventricular myocytes in TAC and Ang-II infusion-induced cardiac hypertrophy.** *A,* average heart weight to body weight (HW/BW) ratio was significantly increased in control WT mice after TAC or Ang-II infusion compared with sham or saline infusion, respectively. *B* and *C,* echocardiography in WT mice reveals a significant decrease in percentage of fractional shortening and ejection fraction in TAC or Ang-II infusion compared with sham or saline infusion respectively. #, $p < 0.05$; *, $p < 0.005$, $n = 8$. *D,* representative Western blot analysis shows reduced Cav-3 protein expression in ventricular myocyte lysates from WT mice after 4 weeks of TAC or Ang-II infusion compared with sham or saline infusion, respectively. *E,* mean Cav-3 expression levels normalized to β-actin levels in TAC- or Ang-II-treated WT mice compared with sham- or saline-treated mice. *, $p < 0.005$, $n = 6$. *F,* representative transmission electron micrographs show reduced number of caveolae in the ventricular myocytes from TAC mice (*upper image*) compared with sham (*lower image*), *scale bar,* 200 nm. *G,* numbers of caveolae estimated as per μm linear lengths of sarcolemmal ventricular myocytes in the TAC mice (199 images) were significantly reduced compared with sham mice (168 images). Data are from five mice in each group, *, $p < 0.005$ compared with sham mice.

us (11). As shown in Fig. 3, a re-expression of $I_{Ca,T}$ (-1.6 ± 0.4 pA/pF) in ventricular myocytes after 4 weeks of TAC compared with negligible current (-0.02 ± 0.05 pA/pF) in ventricular myocytes from sham-treated mice (Fig. 3, *B* and *C*) was observed. In the sham myocytes (Fig. 3*B*), there was no detectable $I_{Ca,T}$ at -30 mV. Similarly, Ang-II infusion resulted in re-expression of $I_{Ca,T}$ in ventricular myocytes (-0.84 ± 0.11 pA/pF) compared with saline-treated animals (-0.19 ± 0.34 pA/pF) (Fig. 3*C*). To confirm the expression of $I_{Ca,T}$ in the WT hypertrophied (TAC) cardiomyocytes, we first measured $I_{Ca,T}$ and then perfused cells with an $I_{Ca,T}$ inhibitor Ni^{2+} (300 μM), which completely abolished the $I_{Ca,T}$ (Fig. 3*E*) but did not significantly impact the $I_{Ca,L}$ (data not shown). The inhibition of $I_{Ca,T}$ by Ni^{2+} confirmed that the Ca^{2+} current elicited at -30 mV is indeed $I_{Ca,T}$. These data confirm that $I_{Ca,T}$ is re-expressed in the ventricular myocytes during TAC- or Ang-II-induced cardiac hypertrophy. $I_{Ca,L}$ was not significantly different in the ventricular myocytes after TAC or Ang-II treatment compared with controls (Fig. 3*D*).

Cardiac-specific Cav-3 Overexpression Attenuates Cardiac Hypertrophy—Recently, we have demonstrated that the cardiac-specific overexpression of Cav-3 resulted in attenuation of

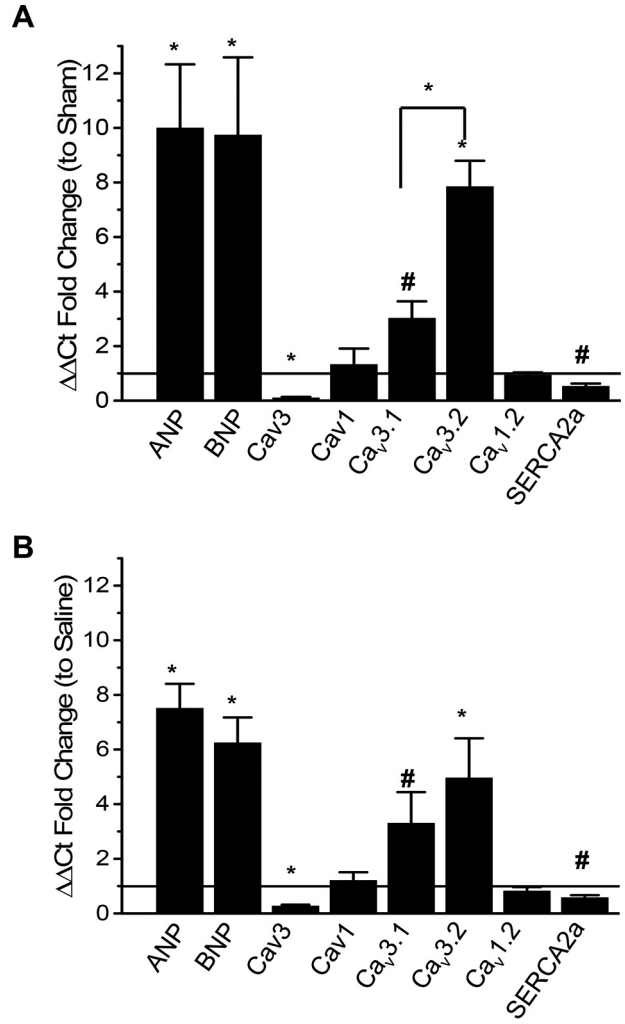

FIGURE 2. **mRNA expression levels using qRT-PCR analysis for genes of interest in TAC- (*A*) or Ang-II infusion (*B*)-induced cardiac hypertrophy.** qRT-PCR analysis shows a significant increase in the atrial natriuretic peptide (*ANP*), brain natriuretic peptide (*BNP*), $Ca_v3.1$ (α_{1G}), and $Ca_v3.2$ (α_{1H}) subunits of the TTCC in hypertrophic left ventricles compared with sham- or saline-treated hearts. The mRNA expression levels for Cav-3 and SERCA2a were significantly reduced, but Cav-1 and $Ca_v1.2$ levels were unchanged in cardiac hypertrophy. Data represent means ± S.E. *, $p < 0.005$; #, $p < 0.05$; $n = 4$.

TAC-induced cardiac hypertrophy via enhanced natriuretic peptide expression (15). Here, we investigated whether Cav-3 OE mice have attenuation of cardiac hypertrophy after Ang-II infusion. Male 12–16-week-old Cav-3 OE and WT mice were subjected to Ang-II or saline infusion or TAC or sham surgery for 4 weeks. As shown in Table 2, echocardiography revealed that WT mice had decreased ejection fraction and percentage fractional shortening after 4 weeks of TAC or continuous Ang-II infusion (Table 2), whereas Cav-3 OE mice subjected to TAC had no change in either measure of cardiac function compared with sham-treated mice. WT mice showed an increase in cardiac hypertrophy in response to TAC or Ang-II infusion with increased ventricular wall thickness and an increase in HW/BW ratio, but TAC or Ang-II infusion in Cav-3 OE mice did not show significant differences in these measures compared with sham or saline treatment, respectively (Table 2). The above data confirm that Cav-3 OE mice are protected from Ang-II-induced cardiac hypertrophy. The data with TAC studies are in agreement with and confirm our previously published results (15).

Caveolin-3 Overexpression Inhibits $I_{Ca,\,T}$ in Cardiac Hypertrophy—A recent study suggested that a re-expression of the $Ca_v3.2$ TTCC current is responsible for the induction of pathological cardiac hypertrophy via calcineurin/NFAT hypertrophic signaling (27). We have shown that Cav-3 overexpression inhibits $Ca_v3.2$ (α_{1H}) channel current but not the $Ca_v3.1$ (α_{1G}) current in mouse neonatal cardiomyocytes (11). Therefore, we hypothesized that ventricular myocytes from Cav-3 OE mice will inhibit re-expression of $I_{Ca,\,T}$, specifically the $I_{Cav3.2}$, and attenuate pressure overload-induced pathological cardiac hypertrophy. We investigated the role of Cav-3 on $I_{Ca,\,T}$ inhibition in pathological hypertrophy using the Cav-3 OE or littermate WT control mice subjected to TAC or Ang-II infusion for 4 weeks. $I_{Ca,\,T}$ and $I_{Ca,\,L}$ were measured in adult ventricular myocytes (AVMs) from mice subjected to different treatment groups. Cell capacitance measured during voltage clamp measurement showed TAC or Ang-II infusion caused 27 and 34% increase, respectively, in the AVM size in the WT mice compared with saline-treated animals (Fig. 4*E*). Cell capacitance of the AVMs from Cav-3 OE mice was 50% greater than AVMs from WT saline-treated mice. TAC or Ang-II infusion did not significantly alter the cell capacitance in AVMs from Cav-3 OE mice (Fig. 4*F*). Peak $I_{Ca,\,T}$, measured at −30 mV normalized to cell capacitance and expressed as pA/pF (Fig. 3*C*), was significantly increased in the AVMs from WT mice after either TAC or Ang-II infusion. $I_{Ca,\,T}$ expression was negligible in saline- and sham-treated WT AVMs (Fig. 3*C*). As shown in Fig. 4, the peak $I_{Ca,\,T}$ was completely inhibited in the AVMs from Cav-3 OE mice after TAC (Fig. 4, *A* and *B*) or Ang-II infusion (Fig. 4*C*), suggesting that cardiac myocyte-specific overexpression of Cav-3 inhibits the TAC- or Ang-II-induced increase in $I_{Ca,\,T}$ during pathological hypertrophy. The peak $I_{Ca,\,L}$ density elicited at 0 mV was not different in the AVMs from mice with all treatment groups (Fig. 4*D*). In addition, the activation and inactivation of $I_{Ca,\,L}$ were not different in the AVMs from mice with all treatment groups (data not shown). The $I_{Ca,\,L}$ data also confirmed our earlier demonstration that Cav-3 overexpression does not alter peak $I_{Ca,\,L}$ density in neonatal mouse ventricular myocytes (11).

Changes in Expression of Key Signaling Proteins in Ventricular Myocytes during Cardiac Hypertrophy—To examine whether the increase in $I_{Ca,\,T}$ expression in hypertrophic myocytes is associated with changes to the protein level for TTCC isoforms $Ca_v3.1$ and $Ca_v3.2$, and other key signaling proteins involved in cardiac hypertrophy, we performed semi-quantitative Western blot analysis on ventricular lysates prepared from WT and Cav-3 OE mice following TAC or sham treatments. As shown in Fig. 5, the expression levels for the $Ca_v3.2$ and PKCα proteins were significantly increased in WT TAC myocytes compared with sham mice. However, the expression levels of $Ca_v3.2$ and PKCα were normalized in the Cav-3 OE hearts following TAC and were not different compared with WT and Cav-3 OE sham hearts. The expression level of $Ca_v3.1$ and PKCβ1 was unchanged in all groups. Also, the Cav-3 overexpression in the hearts (Cav-3 OE mice) did not impact the expression profiles of any of the above proteins. However, the

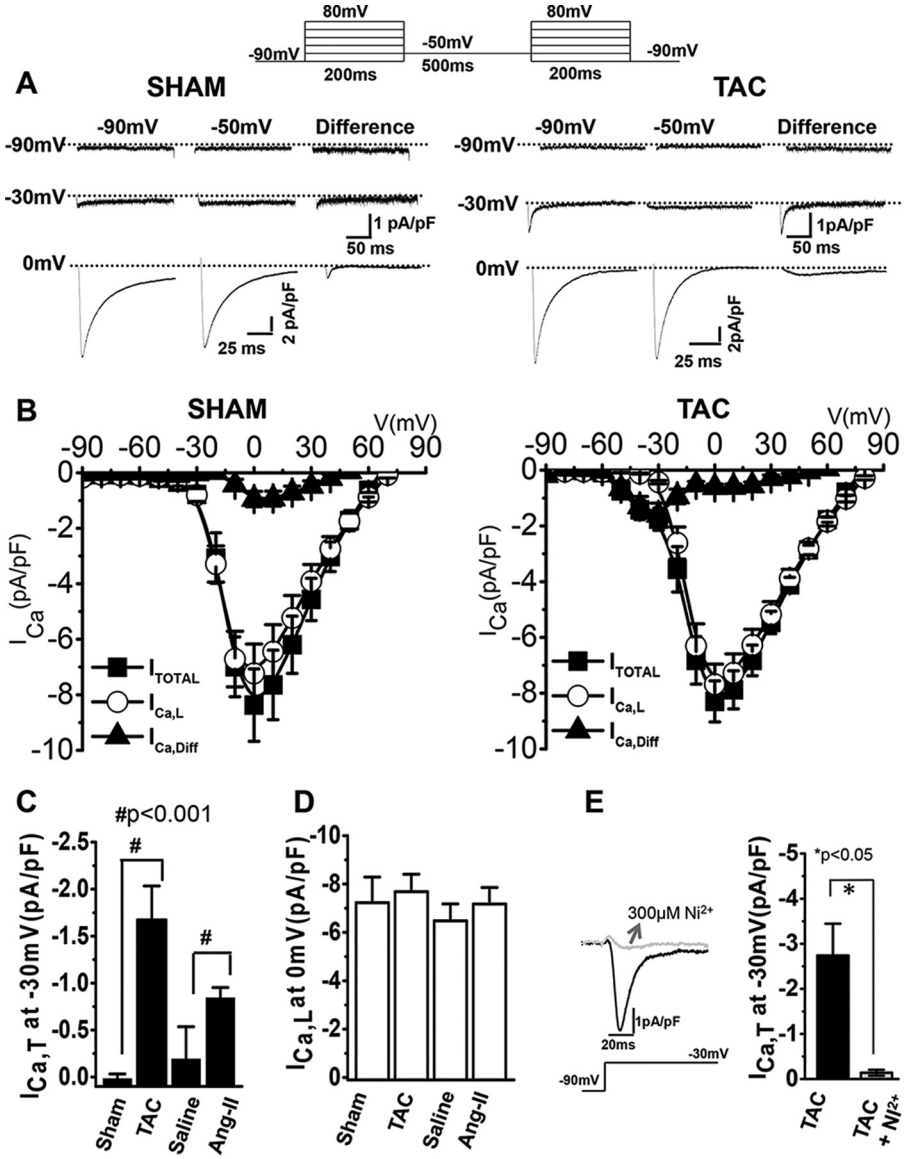

FIGURE 3. **$I_{Ca,T}$ is increased in the left ventricular myocytes from TAC- or Ang-II-infused hypertrophic mice.** *A,* representative calcium current traces were measured using whole cell patch clamp technique in left ventricular myocytes from TAC or sham mice using a dual pulse voltage protocol (*inset*). $I_{Ca,T}$ is referred to as the difference between current recorded between step depolarization at holding potential −90 and −50 mV. *B,* mean current to voltage response of L-type (○) and T-type (▲) current recorded from ventricular myocytes after 4 weeks of TAC or sham in WT mice. *C,* mean peak current densities of $I_{Ca,T}$ at −30 mV were significantly increased in ventricular myocytes from WT mice after 4 weeks of TAC or Ang-II infusion compared with sham or saline infusion, respectively. *D,* mean peak $I_{Ca,L}$ density at 0 mV was unchanged in the ventricular myocytes from WT mice after TAC or sham treatment and Ang-II infusion or saline treatment. $p < 0.001$, $n = 9$ cells from 5 animals in each group. *E,* representative $I_{Ca,T}$ traces from WT TAC myocytes perfused with 300 μM Ni^{2+} (*left*) and mean peak $I_{Ca,T}$ at −30 mV (*right*). $n = 4$ from three animals. Data represent means ± S.E.

TABLE 2

Cardiac-specific Cav-3 overexpression attenuates TAC and Ang-II infusion-induced cardiac hypertrophy

HW/BW indicates ratio of heart weight to body weight; LV mass indicates left ventricular mass; LVPW:d indicates left ventricular posterior wall in diastole; LVID:d indicates left ventricular internal dimension at end diastole; LV/BW, left ventricle/body weight; %FS, % fractional shortening; %ES. % ejection fraction; LVID:d, left ventricular internal diameter end diastole.

	Sham		TAC		Saline		Ang-II	
$n = 8$	WT	Cav-3 OE	WT	Cav-3 OE	WT	Cav-3 OE	WT	Cav-3 OE
Heart rate (beats/min)	496 ± 28	493 ± 19	499 ± 23	511 ± 19	420 ± 21	451 ± 12	461 ± 28	479 ± 10
LV mass (mg)	114.56 ± 8	123 ± 5	156.96 ± 9[a]	132 ± 8	93.63 ± 8	102.4 ± 7	120.9 ± 6	93.57 ± 14
LV/BW	3.35 ± 0.4	3.92 ± 0.5	4.69 ± 0.7[a]	4.24 ± 0.4	3.06 ± 0.1	3.03 ± 0.1	4.08 ± 0.3[a]	3.37 ± 0.3
% FS	34.34 ± 2	33.81 ± 2	25.51 ± 2[a]	31.6 ± 3	32.4 ± 0.5	31.8 ± 0.8	26.6 ± 1[a]	32.6 ± 1
% EF	58.12 ± 2	59.38 ± 3	39.27 ± 3[a]	53.45 ± 5	59.9 ± 2	55.03 ± 3	53.90 ± 2[a]	64.9 ± 3
LVPW:d (mm)	0.74 ± 0.03	0.76 ± 0.02	0.86 ± 0.4[b]	0.73 ± 0.03	0.73 ± 0.1	0.71 ± 0.1	0.85 ± 0.3[a]	0.73 ± 0.01
LVID:d (mm)	4.38 ± 0.5	4.2 ± 0.9	3.27 ± 0.2[b]	3.9 ± 0.8	4.21 ± 0.06	4.21 ± 0.1	3.69 ± 0.1[a]	4.00 ± 0.2

[a] $p < 0.005$.
[b] $p < 0.05$, data ± S.E.

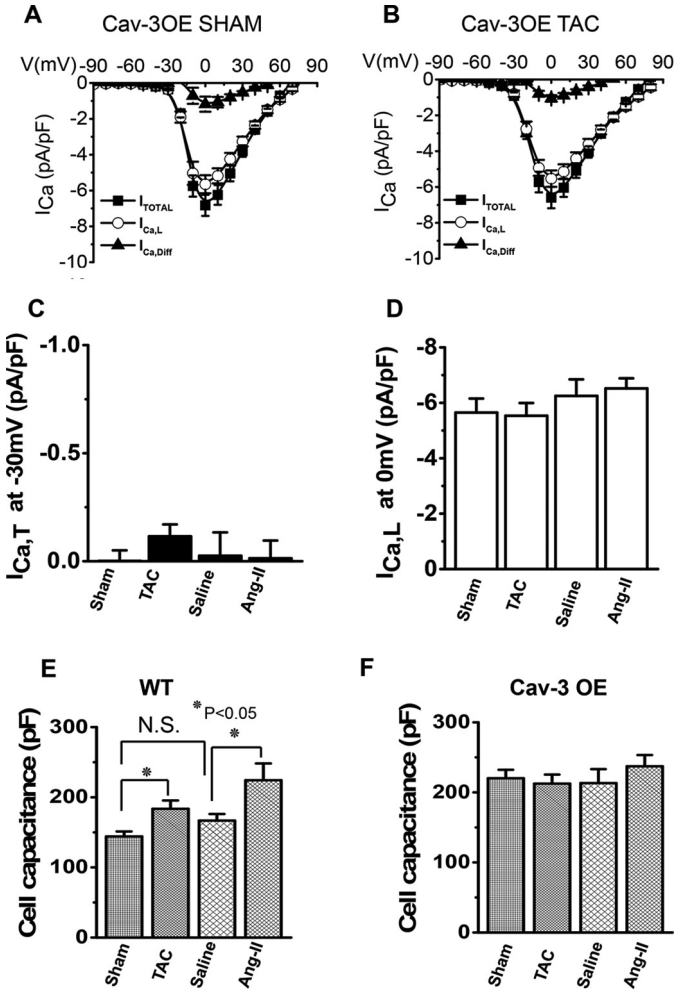

FIGURE 4. **Cardiac-specific Cav-3 OE inhibits $I_{Ca,T}$ in ventricular myocytes from TAC- or Ang-II infusion-induced hypertrophic mice.** *A* and *B,* mean current-voltage response of $I_{Ca,L}$ (○) and $I_{Ca,T}$ (▲) measured from left ventricular myocytes from Cav-3 OE mice after 4 weeks of sham or TAC treatment, respectively. *C,* mean peak $I_{Ca,T}$ density (measured at −30 mV). *D,* mean $I_{Ca,L}$ density (measured at 0 mV) in ventricular myocytes from Cav-3 OE mice after 4 weeks of sham or TAC, and saline or Ang-II infusion were not significantly different. *E,* whole cell membrane capacitance of ventricular myocytes from WT mice subjected to TAC or Ang-II infusion was significantly increased compared with sham or saline infusion, respectively. *F,* whole cell membrane capacitance of ventricular myocytes from Cav-3 OE mice subjected to TAC or Ang-II infusion was not significantly different compared with sham or saline infusion, respectively. Data represent means ± S.E. *, $p < 0.05$, $n = 8–10$ cells from five mice each group. *N.S.,* not significant.

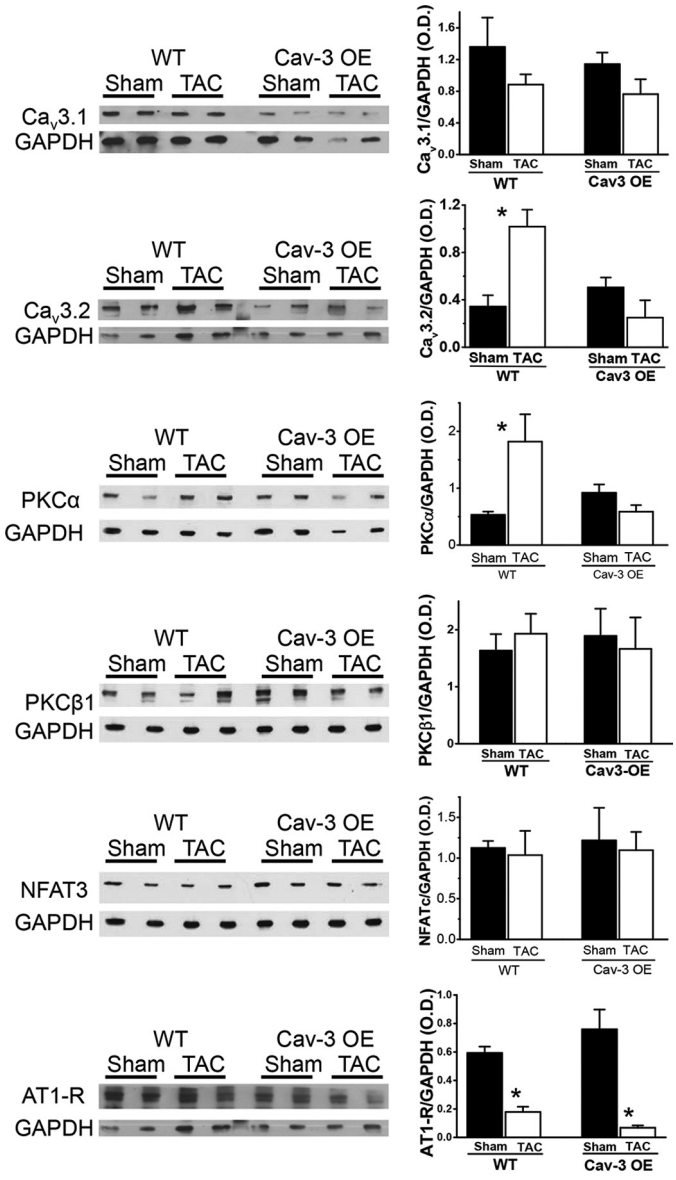

FIGURE 5. **Changes in expression of key signaling protein in ventricular myocytes during cardiac hypertrophy.** Left ventricular myocyte lysates from either WT or Cav-3 OE mice subjected to TAC or sham surgery were separated by SDS-PAGE and Western blot analysis by probing with specific antibodies to $Ca_v3.1$, $Ca_v3.2$, PKCα, PKCβ1, NFATc3, AT1 receptor, and GAPDH. Representative immunoblots indicated for respective proteins and GAPDH signals as loading control are shown on the *left*. The *bar plots* on the *right* show semi-quantitative densitometry analysis for indicated protein expression normalized to GAPDH signals. The expression levels for $Ca_v3.2$ and PKCα were significantly increased in WT TAC hearts compared with WT sham hearts. The AT1 receptor levels were significantly reduced in WT and Cav-3 OE TAC hearts compared with respective sham hearts. (Note that same immunoblot membrane was used to probe for $Ca_v3.2$ and AT1-R and also for PKCβ and NFATc3). Data represents mean ± S.E. $n = 4$ experiments, *, $p < 0.05$.

expression levels for AT-R were significantly reduced in WT and Cav-3 OE hearts following TAC in comparison with sham-treated hearts. These above data indicate that increased expression of the $Ca_v3.2$ and PKCα in cardiac hypertrophy could contribute to an increase in $I_{Ca,T}$ and altered Ca^{2+} signaling.

Cav-3 Overexpression Prevents Disruption of Caveola-associated Macromolecular Signaling Complex—We investigated the impact of reduced Cav-3 and caveola expression on caveola-localized signaling proteins in pathological hypertrophy. Myocyte lysates from mice after 4 weeks of TAC or sham treatment were co-immunoprecipitated (co-IP) using anti-Cav-3 or control IgG antibody. The co-IP samples were analyzed by Western blot by probing with specific antibodies to proteins that are known to associate with Cav-3 such as NOS3, PKCα, and AT1 receptors. Representative Western blots (Fig. 6*A*) show that NOS3, PKCα, and AT1 receptors co-precipitated with Cav-3 from WT or Cav-3 OE myocytes following sham treatment. In contrast, PKCα and AT1 receptor did not co-IP with anti-Cav-3 antibody from TAC myocyte lysates. In contrast, NOS3, a Cav-3 associated protein, was found to co-IP with sham and TAC myocyte lysates. β_1AR, which does not associate with Cav-3, did not co-IP with anti-Cav-3 antibody from sham or TAC myocyte lysates. We then tested whether the overexpression of Cav-3 in the ventricular myocytes from Cav-3 OE mice

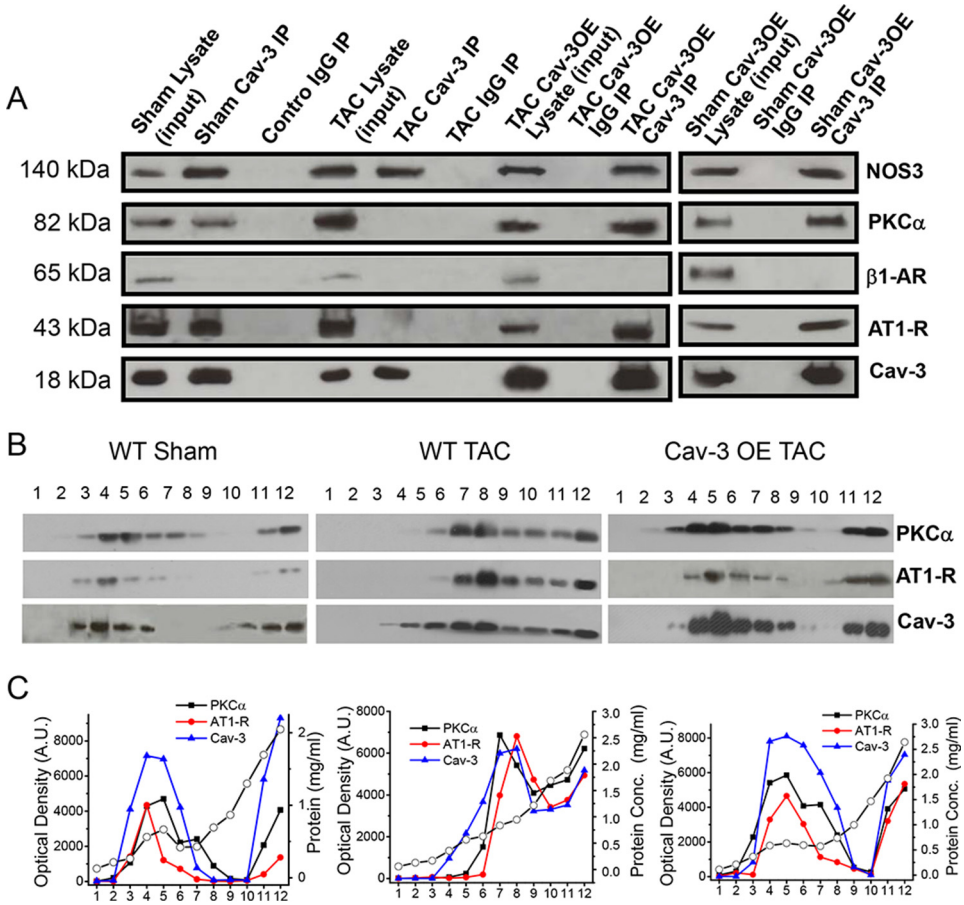

FIGURE 6. **Cardiac-specific Cav-3 OE in mice prevents disruption of caveola-associated macromolecular signaling complexes following TAC-induced cardiac hypertrophy.** Left ventricular myocyte lysates from either WT or Cav-3 OE mice subjected to TAC or sham were used for immunoprecipitation with anti Cav-3 antibody. Immunoprecipitates were separated by Western blot analysis and probed with antibodies to NOS3, β_1AR, PKCα, AT1-R, and Cav-3. Representative immunoblots show NOS3, PKCα, and AT1-R but not the β_1-adrenergic receptor (*β1-AR*) co-immunoprecipitated with anti-Cav-3 antibody from WT sham lysates, whereas control IgG does not immunoprecipitate the proteins (*A*). However, PKCα and AT1-R did not co-IP with anti-Cav-3 from WT TAC myocyte lysates, whereas NOS3 co-immunoprecipitated with Cav-3. In contrast to WT TAC, the NOS3, AT1-R, and PKCα co-immunoprecipitated with anti-Cav-3 from ventricular myocyte lysates from Cav-3 OE mice subjected to TAC. *B,* representative Western blot analysis performed on caveola-enriched membrane fractions prepared using ventricular myocytes from WT sham, WT TAC, and Cav-3 OE TAC hearts. Precipitated proteins from gradient membrane fractions analyzed Western blot by probing with antibodies to PKCα, AT1-R, and Cav-3. *C,* respective plots show relative distribution for PKCα (■), AT1-R (●), and Cav-3 (▲) and protein recovery in each of the gradient fractions as indicated (○). Results are representative of data from two separate experiments.

prevented TAC-induced myocyte remodeling and disruption of caveola-localized signaling proteins. As shown in Fig. 6*A*, PKCα, AT1 receptor, and NOS3 co-IPed with anti-Cav-3 antibody from Cav-3 OE mice subjected to TAC or sham myocytes. To further confirm these above results, we also performed sucrose density membrane fractionation on the WT and Cav-3 OE subjected to TAC or sham surgery and isolated caveola-enriched membrane fractions. As described under "Materials and Methods," equal volumes of the sucrose density gradient membrane fractions were loaded onto SDS-polyacrylamide gels and analyzed by Western blot by probing with antibodies to Cav-3, PKCα, and AT1 receptor. Representative Western blot analysis on the density gradient membrane fractions from WT sham (*left panel*) or WT TAC (*middle panel*) Cav-3 OE TAC-treated hearts is shown in Fig. 6*B*. For the WT sham hearts, the highest enrichment for the Cav-3 signal, indicating enrichment for caveolae, was noticed in the lower density fractions 4–6, as has been reported in many previous studies (18, 28–30). Identical enrichment and distribution for PKCα and AT1 receptor was also detected in the same caveola-enriched fractions (fraction 4–6). The corresponding optical density for the distribution of Cav-3, PKCα, and AT1 receptor is shown in Fig. 6*C* (*left panel*). In contrast, the Cav-3, PKCα, and AT1-receptor distribution was shifted to a higher density gradient fraction (fraction 7 and above; *middle panels*, Fig. 6, *B* and *C*) from WT hearts subjected to TAC suggesting that reduced expression of Cav-3 may have resulted in disruption of caveolae and altered distribution of these signaling proteins. In contrast, the distribution pattern for Cav-3, PKCα, and the AT1 receptor from Cav-3 OE hearts subjected to TAC was similar (Fig. 6, *B* and *C*, *right panels, fractions 4–6*) to that of WT sham hearts (control). The above experiment was repeated to confirm reproducibility of the results. These results suggest that Cav-3 overexpression is associated with reduced TAC-induced myocyte remodeling and decreased disruption of the Cav-3-associated macromolecular signaling complexes.

Cav-3 Knockdown Results in Increased Ang-II Stimulation of $I_{Ca,\,T}$ Mediated by PKCα in Neonatal Mouse Ventricular Myocytes—To further investigate the impact of reduced Cav-3 expression and mechanism of increased $I_{Ca,\,T}$ in Ang-II-medi-

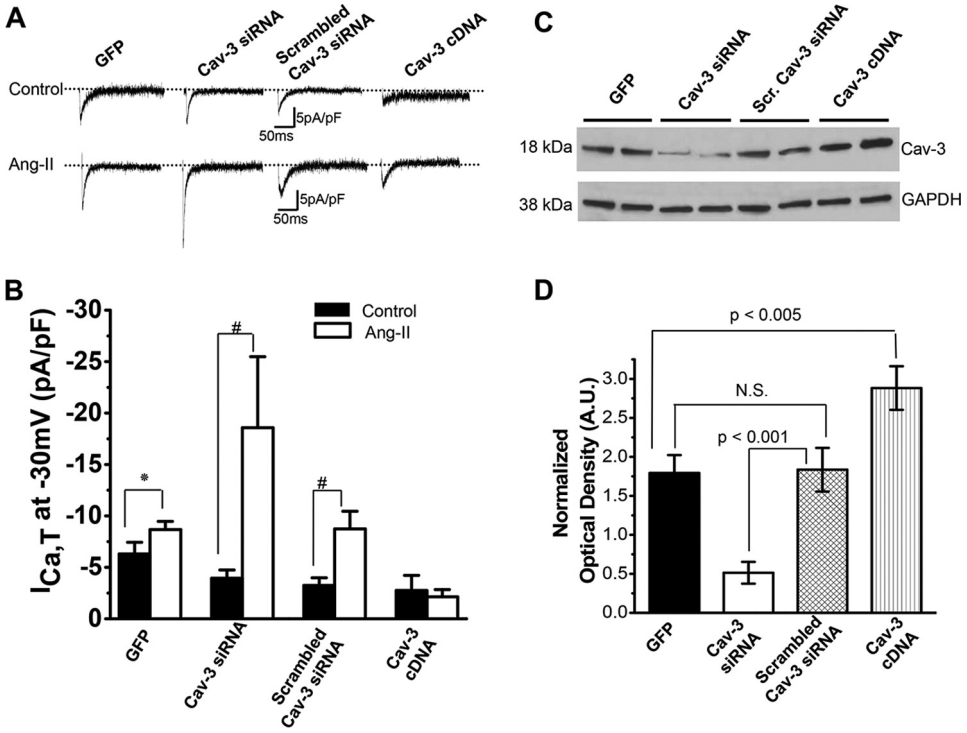

FIGURE 7. **siRNA-mediated knockdown of Cav-3 expression increases Ang-II stimulation of $I_{Ca,T}$ in neonatal mouse ventricular myocytes.** NMVMs were transfected with either eGFP alone, Cav-3 siRNA + eGFP, scrambled Cav-3 siRNA+ eGFP, and Cav-3 cDNA + eGFP. $I_{Ca,T}$ was measured using a dual pulse protocol as described under "Materials and Methods." *A,* representative peak $I_{Ca,T}$ traces (at −30 mV) recorded from NMVMs that were transfected as indicated and treated with vehicle (control) or Ang-II (10 μmol/liter for 48 h). *B,* mean peak $I_{Ca,T}$ in NMVMs. Ang-II treatment caused significant increase in the $I_{Ca,T}$ (*, $p < 0.05$). Cav-3 siRNA caused a further robust increase in the Ang-II stimulation of peak $I_{Ca,T}$ (#, $p < 0.005$). Scrambled Cav-3 siRNA, used as control, also significantly increased $I_{Ca,T}$ compared with vehicle (#, $p < 0.005$). Basal and Ang-II stimulation of $I_{Ca,T}$ was significantly inhibited in NMVMs transfected with Cav-3 cDNA compared with control treatment (*, $p < 0.05$). Data represent means ± S.E.; $n = 5$–7 cells from three separate transfections. *C,* representative Western blots show protein expression for Cav-3 and GAPDH in NMVMs. *D,* semi-quantitative densitometry analysis for Cav-3 expression normalized to GAPDH signals. siRNA-mediated knockdown of Cav-3 caused a significant reduction in the expression of Cav-3 in the NMVMs compared with control scrambled siRNA-transfected cells ($p < 0.001$). The NMVMs transfected with Cav-3 cDNA showed significantly higher Cav-3 expression compared with eGFP ($p < 0.005$). Data represent means ± S.E., $n = 6$.

ated cardiac hypertrophy, we used cultured NMVMs, which are known to endogenously express the $I_{Ca,T}$ (11, 31, 32). Cultured NMVMs were treated with Ang-II (10 μmol/liter) or vehicle for 48 h, and $I_{Ca,T}$ was measured. As shown in Fig. 7, *A* and *B*, Ang-II treatment caused a significant increase (38%) in the peak $I_{Ca,T}$ (−8.7 ± 0.8 pA/pF) compared with control (−6.3 ± 1.1 pA/pF) NMVMs. In separate experiments using NMVMs, we performed siRNA-mediated knockdown of Cav-3 using specific siRNA oligonucleotides to Cav-3 or overexpression of Cav-3 using cDNA of Cav-3 as described previously (11). siRNA-mediated knockdown of Cav-3 or overexpression of Cav-3 was confirmed by Western blot analysis (Fig. 7, *C* and *D*). As shown in Fig. 7, *A* and *B*, siRNA-mediated knockdown of Cav-3 further enhanced (112%) Ang-II stimulation of peak $I_{Ca,T}$ (−18.6 ± 7 pA/pF) compared with scrambled Cav-3 siRNA (−7 ± 0.8 pA/PF) or vehicle-treated NMVMs (−3.9 ± 0.8 pA/pF; 372%). In contrast, Cav-3 overexpression inhibited the basal peak $I_{Ca,T}$ and abolished the Ang-II stimulation of peak $I_{Ca,T}$ (−2 ± 0.7 pA/pF). Previous studies have demonstrated that PKCα activates and regulates the $Ca_v3.2$ channel current (33, 34). Increased PKCα expression and signaling were reported in cardiac hypertrophy and heart failure (35, 36). Chronic activation of the renin angiotensin system is known to induce cardiac hypertrophy, and Ang-II stimulation of cardiomyocytes causes increase in $I_{Ca,T}$ in a PKC-dependent fashion (37, 38). We rationalized that with reduced expression of Cav-3, PKCα may couple to the $Ca_v3.2$ channels resulting in an enhanced regulation of the $I_{Ca,T}$ in the myocytes. To test this, we performed knockdown of the PKCα using specific shRNA. The NMVMs were co-transfected with eGFP and either Cav-3 siRNA + shRNA PKCα, scrambled Cav-3 siRNA + shRNA PKCα, scrambled Cav-3 siRNA + empty vector, Cav-3 + shRNA PKCα, or Cav-3 + empty vector. Knockdown of the PKCα or Cav-3 or overexpression of Cav-3 was confirmed by semi-quantitative Western blot analysis as shown in Fig. 8, *C* and *D*. The transfected myocytes were treated with vehicle and Ang-II (10 μmol/liter) for 48 h, and $I_{Ca,T}$ was measured in single cells expressing GFP. The knockdown of PKCα completely abolished the Ang-II stimulation of peak $I_{Ca,T}$ (−1 ± 0.37 pA/pF) compared with Ang-II stimulation of peak $I_{Ca,T}$ (−21.8 ± 4.6 pA/pF) (Fig. 8, *A* and *B*). Interestingly, knockdown of PKCα did not impact the peak $I_{Ca,T}$ in the vehicle-treated control NMVMs (4.6 ± 1 pA/pF) compared with vehicle-treated NMVMs transfected with GFP alone (−6.3 ± 1.1 pA/pF) or scrambled Cav-3 siRNA (−6.3 ± 3.7 pA/pF), indicating that PKCα did not regulate the basal $I_{Ca,T}$ currents in the NMVMs. These data clearly suggest that the Ang-II stimulation of the $I_{Ca,T}$ is specifically mediated by PKCα in the NMVMs. Moreover, in NMVMs co-transfected with shRNA to PKCα and Cav-3 cDNA, the basal (vehicle-treated) and Ang-II-stimulated $I_{Ca,T}$

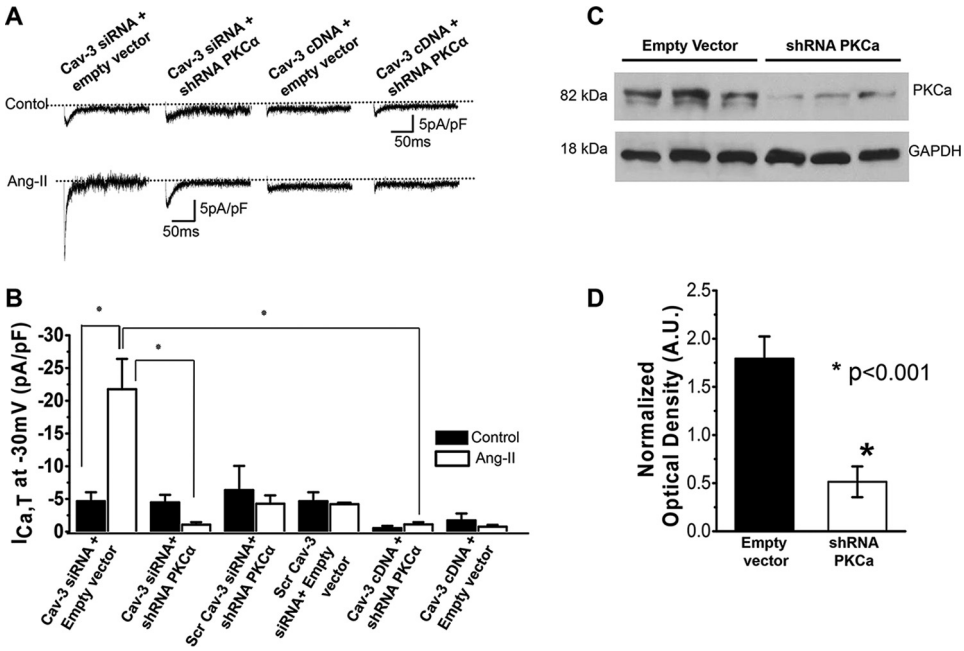

FIGURE 8. **Cav-3 overexpression prevents PKCα-mediated Ang-II stimulation of $I_{Ca,T}$ in neonatal mouse ventricular myocytes.** NMVMs were transfected with either Cav-3 siRNA or scrambled (*scr*) sequence of Cav-3 siRNA as control, or shRNA to PKCα or cDNA plasmid of Cav-3. $I_{Ca,T}$ was measured in the NMVMs transfected as indicated. *A,* representative peak $I_{Ca,T}$ traces from vehicle control or Ang-II-treated (10μmol/liter for 48 h) NMVMs transfected as indicated on *top*. *B,* mean peak $I_{Ca,T}$, measured at −30 mV in NMVMs with vehicle or Ang-II treatment. siRNA-mediated Cav-3 knockdown resulted in significant increase in the Ang-II stimulation of $I_{Ca,T}$ compared with control. shRNA-mediated knockdown of PKCα and Cav-3 overexpression completely inhibited the basal and Ang-II stimulation of $I_{Ca,T}$. *, $p < 0.005$, data ± S.E., $n = 6–8$ cells from three separate experiments. *C,* representative Western blots show protein expression for PKCα and GAPDH in transfected NMVMs. *D,* semi-quantitative densitometry analysis for PKCα expression normalized to GAPDH signals. shRNA-mediated knockdown of PKCα caused a significant reduction in the expression of PKCα in the NMVMs compared with control vector-transfected cells ($p < 0.001$). Data represent means ± S.E., $n = 6$.

were significantly reduced (vehicle −0.55 ± 1 pA/pF *versus* Ang-II −1.1 ± 0.5 pA/pF). These data suggest that Cav-3 overexpression inhibits both the basal and Ang-II stimulation of the $I_{Ca,T}$ that is mediated by the PKCα. These above measurements were performed using a dual pulse protocol as described under "Materials and Methods," which allowed us to also record the $I_{Ca,L}$ density in the NMVMs under various treatment conditions. Importantly, the Ang-II treatment did not alter peak $I_{Ca,L}$ density compared with vehicle (control)-treated NMVMs. In addition, the peak $I_{Ca,L}$ density was unchanged following siRNA-mediated knockdown of Cav-3 or shRNA-mediated knockdown of PKCα or with Cav-3 overexpression in any of the treatment groups (data not shown). Taken together, our results strongly suggest that knockdown of Cav-3 results in enhanced Ang-II stimulation of the $I_{Ca,T}$, whereas overexpression of Cav-3 abrogates both basal and PKCα mediated Ang-II stimulation of the $I_{Ca,T}$.

Cav-3 Overexpression Attenuates the Activation of Calcineurin/NFAT Signaling in Neonatal Ventricular Myocytes—The activation of the Ca^{2+}-dependent calcineurin-NFAT signaling pathway is involved in Ang-II-induced pathological cardiac hypertrophy (39, 40). We hypothesized that the enhanced $I_{Ca,T}$ due to reduced Cav-3 expression will activate the Ca^{2+}-dependent calcineurin/NFAT signaling following Ang-II stimulation, and this effect can be reversed with stable Cav-3 expression. We tested our hypothesis in the cultured NMVMs by transfecting with either Cav-3 siRNA or scrambled control Cav-3 siRNA or cDNA to Cav-3 (Cav-3 overexpression) and co-transfected with m-Cherry. After 24 h in culture, the NMVMs were infected with NFATc3-GFP adenovirus (gift from Dr. Steve Houser, Temple University). Cells were then treated with Ang-II or vehicle in the presence of 4 mmol/liter extracellular Ca^{2+}. 24 h later, NMVMs were stained with the nuclear stain DAPI and imaged under a confocal microscope to determine cytoplasm *versus* nuclear localization of the NFATc3-GFP signal. As shown in representative images (Fig. 9*A*), in the vehicle-treated control NMVMs, almost the entire NFATc3-GFP signal was observed in the cytoplasm. In contrast, Ang-II treatment caused significant nuclear translocation of NFATc3-GFP in 75% ($p < 0.05$; Fig. 9*B*) of the cells. Similarly, Ang-II treatment in NMVMs caused NFATc3-GFP translocation into the nucleus in 87.5% of NMVMs ($p < 0.05$; Fig. 9*B*), where Cav-3 was knocked down by specific siRNA. However, in NMVMs overexpressing Cav-3, the nuclear translocation of NFATc3-GFP was almost completely inhibited (only 5% of cells showed nuclear localization of NFATc3-GFP) upon treatment with Ang-II, which was similar to the cells treated with vehicle. Interestingly, Cav-3 knockdown alone did not cause nuclear translocation of the NFATc3-GFP. These data show that Cav-3 overexpression prevents nuclear translocation of the NFATc3-GFP upon Ang-II stimulation. Taken together, these data suggest that Cav-3 overexpression prevents local increase in the Ca^{2+} levels via inhibition of Ang-II stimulation of $I_{Ca,T}$, and it thereby prevents activation of the calcineurin/NFAT signaling.

Discussion

This study investigated whether and how a loss of Cav-3 in pressure overload-induced cardiac hypertrophy impacts myocyte Ca^{2+} signaling and leads to pathological cardiac hypertro-

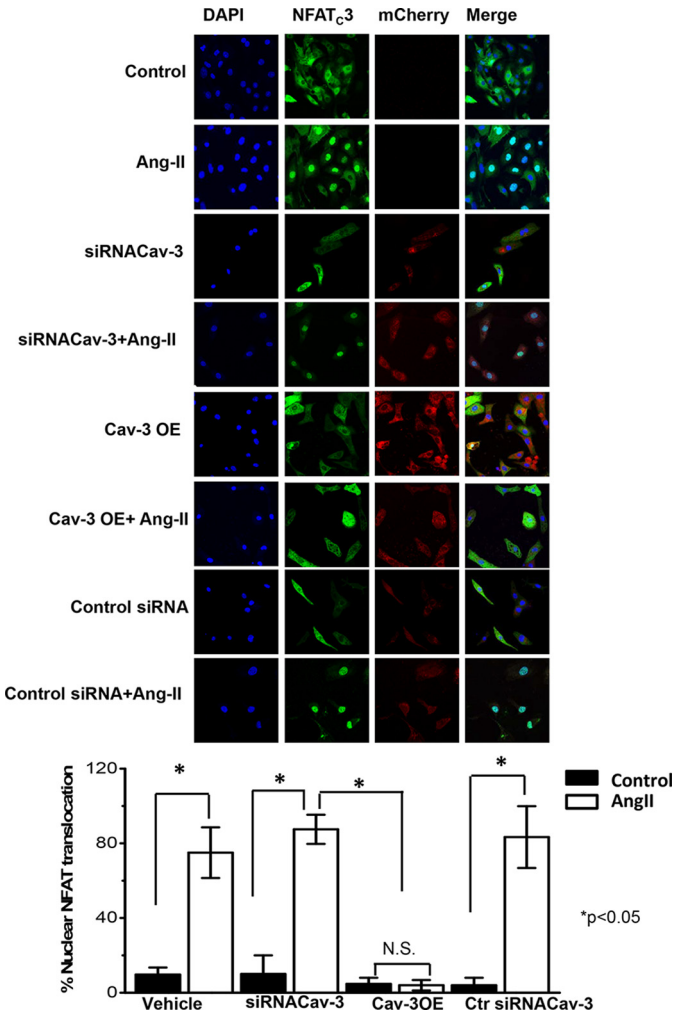

FIGURE 9. **Overexpression of Cav-3 inhibits Ang-II-induced NFATc3-GFP translocation to nucleus.** Representative images of NMVMs showing localization NFATc3-GFP following vehicle (control) or Ang-II treatment. Freshly isolated NMVMs were transfected with Cav-3 siRNA or Cav-3 cDNA plasmid, grown in culture for 12 h, and then infected with NFATc3-GFP adenovirus. 24 h after infection, the cells were treated with vehicle (control) or Ang-II (10μmol/liter), and the culture media were supplemented with 4 mmol/liter Ca^{2+}. GFP-tagged NFAT-C3-infected NMVMs were co-stained with nuclear stain DAPI (*blue*) and m-Cherry as transfection control. 24 h of Ang-II treatment caused a nuclear translocation of NFATc3-GFP compared with control. siRNA-mediated Cav-3 knockdown caused nuclear translocation of NFATc3-GFP in nearly all of NMVMs. In contrast, the NMVMs overexpressing Cav-3 nuclear translocation of NFATc3-GFP was completely inhibited. *Scale bar,* 50 μm. Data are representative of four separate experiments. *N.S.,* not significant.

phy. The results presented here highlight several novel and important findings. We show reduced Cav-3 expression and abundance of caveolae and a simultaneous increase in the $Ca_v3.2$ protein and $I_{Ca,\,T}$ in the ventricular myocytes in cardiac hypertrophy. Reduced Cav-3 expression resulted in dissociation of the AT1 receptor and PKCα from Cav-3 in the hypertrophic ventricular myocytes. In NMVMs, siRNA-mediated knockdown of Cav-3 results in increased Ang-II stimulation of $I_{Ca,\,T}$ mediated by PKCα and caused calcineurin-dependent NFAT translocation into the nucleus. In contrast, Cav-3 overexpression inhibited the PKCα-mediated Ang-II stimulation of the $I_{Ca,\,T}$ and prevented NFATc3 translocation into the nucleus. In addition, mice with cardiac-specific Cav-3 overexpression had reduced expression of $I_{Ca,\,T}$ and prevented disruption of the Cav-3-associated macromolecular signaling complexes after exposure to cardiac hypertrophic stimuli. Taken together, our data demonstrate that Cav-3 overexpression protects against pressure overload-induced cardiac hypertrophy via inhibition of $I_{Ca,\,T}$ and suppression of the Ca^{2+}-dependent hypertrophic calcineurin-NFAT signaling pathway.

Previous work (15) and current investigations demonstrate that caveola and Cav-3 expression is essential to cardiac protection (anti-hypertrophic signaling). The reduced Cav-3 expression in the cardiomyocytes during cardiac hypertrophy (Fig. 1) is consistent with previously published results (13, 20). Besides a variety of signaling proteins, Cav-3 associates and localizes the $Ca_v3.2$ channels, AT1 receptor, and the PKC isoforms into caveolae and provides local regulation of Ca^{2+} signaling in the cardiomyocytes (9). During pathological remodeling of myocardium, the structural integrity of myocytes is altered, resulting in changes in the distribution of the ion channels and associated signaling proteins, which causes a loss of protein-protein interaction (41). A reduction in Cav-3 expression and reduced abundance of caveolae in cardiomyocytes in cardiac hypertrophy could lead to altered subcellular localization and changes in composition of caveola-associated macromolecular signaling proteins. Previous studies have demonstrated that caveolar localization of key signaling proteins, including soluble guanylyl cyclase and cGMP-dependent protein kinase, is disrupted during pressure (30) or volume overload (29)-induced cardiac hypertrophy. The latter study also showed that caveolar localization protected soluble guanylyl cyclase against oxidation. It was shown that Cav-3 knockdown prevented the redistribution of $5\text{-}HT_{2A}$ receptors into caveolar domains (20). Similarly, our data show that Cav-3, AT-1 receptor, and PKCα were associated and formed a macromolecular signaling complex in normal cardiomyocytes, which was disrupted by a loss of Cav-3 and caveola expression in the hypertrophic ventricular myocytes (Fig. 6). The loss of Cav-3 expression and combined with an up-regulation of the PKCα and dissociation of PKCα from Cav-3 augmented enhanced coupling of PKCα with the $Ca_v3.2$ channels resulting in increased Ang-II stimulation of the $I_{Ca,\,T}$. In contrast, the overexpression of Cav-3 reversed these effects. Therefore, we propose that caveolae provide a safety mechanism against activation of hypertrophic signaling. Re-expression of fetal $I_{Ca,\,T}$ in the ventricular myocytes during pathological hypertrophy is well established (22, 23, 42). Studies have demonstrated the expression of the $Ca_v3.2$ (α_{1H}) channel current responsible for the development of cardiac hypertrophy (27, 44) and the expression of the $Ca_v3.1$ (α_{1G}) channels is attributed to anti-hypertrophic effect and cardioprotective function (45). It was reported that in pathological hypertrophy the Ca^{2+} influx via the re-expressed $Ca_v3.2$ channel initiates the binding of calcineurin to the C terminus of $Ca_v3.2$ leading to activation of NFAT (46). Furthermore, treatment with TTCC blockers could prevent the development of cardiac hypertrophy and heart failure (27, 47, 48). We have recently demonstrated that both the cardiac TTCC isoforms, $Ca_v3.1$ and $Ca_v3.2$ subunits, are associated with Cav-3. However, Cav-3 specifically inhibits the $Ca_v3.2$ current but not the $Ca_v3.1$ cur-

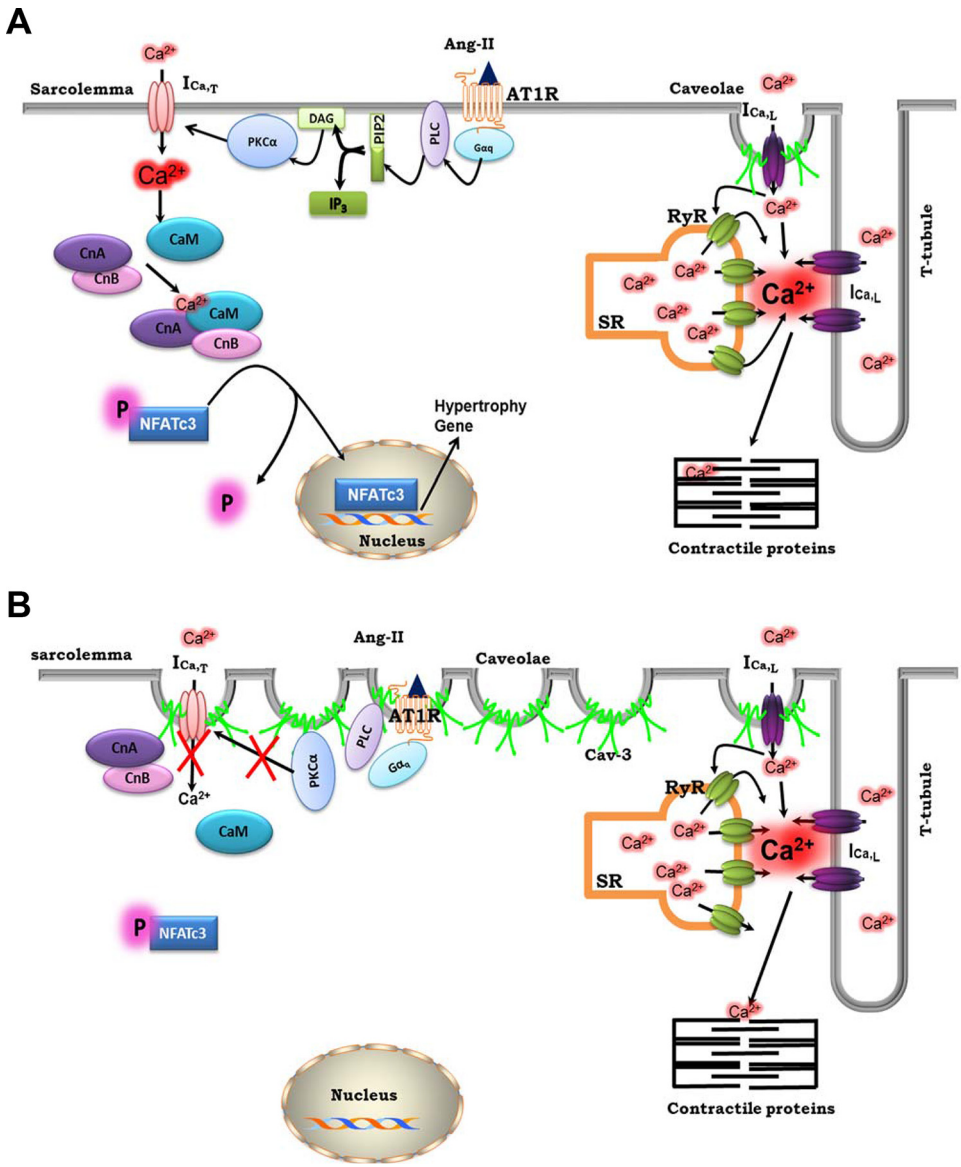

FIGURE 10. **Proposed model of Cav-3-mediated cardiac protection during cardiac hypertrophy.** *A,* during pressure overload-induced cardiac hypertrophy, a reduced expression of Cav-3 and caveola leads to disruption of caveola-localized and Cav-3-associated signaling proteins, including the AT1-R and PKCα. As a result, an increased Ang-II stimulation and PKCα-mediated activation of the $I_{Ca,T}$ lead to an increase in the local intracellular Ca^{2+} levels. This enhanced Ca^{2+} then activates the calmodulin-sensitive calcineurin, which then dephosphorylates NFATc3 triggering a hypertrophic response. However, in *model B* Cav-3 overexpression inhibits $I_{Ca,T}$ and prevents up-regulation of local Ca^{2+} levels and prevents activation of downstream calcineurin/NFATc3 signaling. Cav-3 overexpression also causes caveola formation, which may stabilize the Cav-3-associated macromolecular signaling proteins and therefore protects against pressure overload-induced cardiac hypertrophy.

rents (11). These above reports, including ours, suggest a likely scenario of $Ca_v3.1$ and $Ca_v3.2$ channels activating different signaling pathways within the same caveola via specific coupling mechanisms with different signaling proteins. In this study, we show an increase in the mRNA level for $Ca_v3.1$ (α_{1G}) and $Ca_v3.2$ (α_{1H}) mRNA (Fig. 2) and protein (Fig. 5) and an increase in the $I_{Ca,T}$ in cardiac hypertrophy. We could not specifically measure the contribution of $I_{Cav3.2}$ *versus* $I_{Cav3.1}$ in the cardiomyocytes during hypertrophy due to nonavailability of specific inhibitors for these TTCC isoforms. Interestingly, we did not observe any changes to the $I_{Ca,L}$ density in cardiomyocytes in cardiac hypertrophy in the WT or the Cav-3 OE mice (Figs. 3*D* and 4*D*). Some studies reported a reduction or no change or an increase in the $I_{Ca,L}$ density in hypertrophy (49, 50), whereas other reports suggested a role for the LTCC current in the pathological hypertrophy (51, 52). A recent report indicates that caveola-localized LTCC can activate the calcineurin/NFAT-mediated hypertrophic signaling in cardiomyocytes (53). Subsequently, it was shown that Ca^{2+} influx through LTCCs primarily activates the Cn-NFAT signaling, and Ca^{2+} entry through transient receptor potential (TRP) channels also participated in this process (54). An earlier report indicated that TRP channels as necessary mediators of pathological cardiac hypertrophy through a calcineurin-NFAT signaling pathway (55). Although the TRP3 channel has been shown to localize to caveolae in the arterial smooth muscle cells (17), it is not known whether the TRP channels are associated with caveolar signaling proteins in the ventricular myocytes. We did not examine the role of Cav-3 in

regulation TRP channel currents. Our data clearly suggest that cardiomyocyte caveolae localize essential signals that regulate the Ca^{2+} influx-mediated hypertrophic signaling. Likely differences between our observations of unchanged $I_{Ca,\,L}$ density with other studies could be due to differences in the models of pathological cardiac hypertrophy (early stage) *versus* heart failure (43). Future studies should investigate a clear role for the $Ca_v1.2$ channels, including the expression of auxiliary subunits and isoforms during the development of pathological cardiac hypertrophy and heart failure. Nevertheless, this study clearly establishes the essential protective function of Cav-3 and caveolae in the regulation of Ca^{2+}-dependent signaling mechanisms in pathological hypertrophy.

Conclusion

We demonstrate that the loss of Cav-3 and caveola expression in ventricular myocytes in cardiac hypertrophy impacts the Cav-3-mediated compartmentalized regulation of local signaling. A loss of Cav-3 inhibition of the $I_{Ca,\,T}$, specifically the $I_{Ca\,v3.2}$, results in increased local intracellular Ca^{2+} levels that activate calmodulin-dependent calcineurin, which then dephosphorylates the NFAT and triggers hypertrophic responses (Fig. 10*A*). In contrast, Cav-3 overexpression in the ventricular myocytes prevents pressure overload-induced cardiac hypertrophy via at least two possible mechanisms. Overexpression of Cav-3 directly inhibits $I_{Ca,\,T}$ and prevents an increase in microdomain Ca^{2+} levels. Next. Cav-3 stabilizes the caveola-localized macromolecular signaling complexes and prevents increased coupling of PKCα with the $Ca_v3.2$ channels (Fig. 10*B*). We conclude that Cav-3 overexpression in ventricular myocytes is essential for promoting the protective signaling during pressure overload-induced cardiac hypertrophy and thus could be used as therapeutic strategy for treatment of such disease.

Author Contributions—Y. S. M. conceived, performed, analyzed the experiments in Figs. 3, 4, and 7–10, and wrote the paper. L. J. P. performed the experiments in Figs. 1 and 10. M. T. W. and C. R. R. performed the experiments in Figs. 2, 7, *C* and *D*, and 8, *C* and *D*. A. M. K. and C. R. R. performed the experiments in Fig. 5 and analyzed data. B. K. A. helped perform the experiments in Fig. 1*F*. T. A. H. performed and analyzed the experiments in Table 2 and Fig. 1, *A*–*C*. D. M. R. and H. H. P. provided technical assistance, provided transgenic animals, and edited the manuscript. R. C. B. performed the experiments in Figs. 1, *D* and *E*, and 6, conceived and coordinated the study, analyzed the data, and wrote the paper.

Acknowledgments—We thank Dr. Steven Houser, Temple University, for generously providing adenovirus NFATc3-GFP and Dr. Scott Kaufmann, Mayo Clinic, Rochester, MN, for providing PKCα shRNA plasmid.

References

1. Levy, D., Anderson, K. M., Savage, D. D., Balkus, S. A., Kannel, W. B., and Castelli, W. P. (1987) Risk of ventricular arrhythmias in left ventricular hypertrophy: the Framingham Heart Study. *Am. J. Cardiol.* **60,** 560–565
2. Perrino, C., Naga Prasad, S. V., Mao, L., Noma, T., Yan, Z., Kim, H. S., Smithies, O., and Rockman, H. A. (2006) Intermittent pressure overload triggers hypertrophy-independent cardiac dysfunction and vascular rarefaction. *J. Clin. Invest.* **116,** 1547–1560
3. Frey, N., and Olson, E. N. (2003) Cardiac hypertrophy: the good, the bad, and the ugly. *Annu. Rev. Physiol.* **65,** 45–79
4. Houser, S. R., and Molkentin, J. D. (2008) Does contractile Ca^{2+} control calcineurin-NFAT signaling and pathological hypertrophy in cardiac myocytes? *Sci. Signal.* **1,** pe31
5. Goonasekera, S. A., and Molkentin, J. D. (2012) Unraveling the secrets of a double life: contractile *versus* signaling Ca^{2+} in a cardiac myocyte. *J. Mol. Cell. Cardiol.* **52,** 317–322
6. Wei, S., Guo, A., Chen, B., Kutschke, W., Xie, Y. P., Zimmerman, K., Weiss, R. M., Anderson, M. E., Cheng, H., and Song, L. S. (2010) T-tubule remodeling during transition from hypertrophy to heart failure. *Circ. Res.* **107,** 520–531
7. Balijepalli, R. C., Lokuta, A. J., Maertz, N. A., Buck, J. M., Haworth, R. A., Valdivia, H. H., and Kamp, T. J. (2003) Depletion of T-tubules and specific subcellular changes in sarcolemmal proteins in tachycardia-induced heart failure. *Cardiovasc. Res.* **59,** 67–77
8. Lyon, A. R., MacLeod, K. T., Zhang, Y., Garcia, E., Kanda, G. K., Lab, M. J., Korchev, Y. E., Harding, S. E., and Gorelik, J. (2009) Loss of T-tubules and other changes to surface topography in ventricular myocytes from failing human and rat heart. *Proc. Natl. Acad. Sci. U.S.A.* **106,** 6854–6859
9. Patel, H. H., Murray, F., and Insel, P. A. (2008) G-protein-coupled receptor-signaling components in membrane raft and caveolae microdomains. *Handb. Exp. Pharmacol.* **186,** 167–184
10. Balijepalli, R. C., and Kamp, T. J. (2008) Caveolae, ion channels and cardiac arrhythmias. *Prog. Biophys. Mol. Biol.* **98,** 149–160
11. Markandeya, Y. S., Fahey, J. M., Pluteanu, F., Cribbs, L. L., and Balijepalli, R. C. (2011) Caveolin-3 regulates protein kinase A modulation of the Ca(V)3.2 (α1H) T-type Ca^{2+} channels. *J. Biol. Chem.* **286,** 2433–2444
12. Williams, T. M., and Lisanti, M. P. (2004) The caveolin genes: from cell biology to medicine. *Ann. Med.* **36,** 584–595
13. Feiner, E. C., Chung, P., Jasmin, J. F., Zhang, J., Whitaker-Menezes, D., Myers, V., Song, J., Feldman, E. W., Funakoshi, H., Degeorge, B. R., Jr., Yelamarty, R. V., Koch, W. J., Lisanti, M. P., McTiernan, C. F., Cheung, J. Y., *et al.* (2011) Left ventricular dysfunction in murine models of heart failure and in failing human heart is associated with a selective decrease in the expression of caveolin-3. *J. Card. Fail.* **17,** 253–263
14. Tsutsumi, Y. M., Horikawa, Y. T., Jennings, M. M., Kidd, M. W., Niesman, I. R., Yokoyama, U., Head, B. P., Hagiwara, Y., Ishikawa, Y., Miyanohara, A., Patel, P. M., Insel, P. A., Patel, H. H., and Roth, D. M. (2008) Cardiac-specific overexpression of caveolin-3 induces endogenous cardiac protection by mimicking ischemic preconditioning. *Circulation* **118,** 1979–1988
15. Horikawa, Y. T., Panneerselvam, M., Kawaraguchi, Y., Tsutsumi, Y. M., Ali, S. S., Balijepalli, R. C., Murray, F., Head, B. P., Niesman, I. R., Rieg, T., Vallon, V., Insel, P. A., Patel, H. H., and Roth, D. M. (2011) Cardiac-specific overexpression of caveolin-3 attenuates cardiac hypertrophy and increases natriuretic peptide expression and signaling. *J. Am. Coll. Cardiol.* **57,** 2273–2283
16. Rockman, H. A., Ross, R. S., Harris, A. N., Knowlton, K. U., Steinhelper, M. E., Field, L. J., Ross, J., Jr., and Chien, K. R. (1991) Segregation of atrial-specific and inducible expression of an atrial natriuretic factor transgene in an *in vivo* murine model of cardiac hypertrophy. *Proc. Natl. Acad. Sci. U.S.A.* **88,** 8277–8281
17. Adebiyi, A., Narayanan, D., and Jaggar, J. H. (2011) Caveolin-1 assembles type 1 inositol 1,4,5-trisphosphate receptors and canonical transient receptor potential 3 channels into a functional signaling complex in arterial smooth muscle cells. *J. Biol. Chem.* **286,** 4341–4348
18. Balijepalli, R. C., Foell, J. D., Hall, D. D., Hell, J. W., and Kamp, T. J. (2006) Localization of cardiac L-type Ca^{2+} channels to a caveolar macromolecular signaling complex is required for β2-adrenergic regulation. *Proc. Natl. Acad. Sci. U.S.A.* **103,** 7500–7505
19. Meng, X. W., Heldebrant, M. P., Flatten, K. S., Loegering, D. A., Dai, H., Schneider, P. A., Gomez, T. S., Peterson, K. L., Trushin, S. A., Hess, A. D., Smith, B. D., Karp, J. E., Billadeau, D. D., and Kaufmann, S. H. (2010) Protein kinase Cβ modulates ligand-induced cell surface death receptor

accumulation: a mechanistic basis for enzastaurin-death ligand synergy. *J. Biol. Chem.* **285,** 888–902
20. Mialet-Perez, J., D'Angelo, R., Villeneuve, C., Ordener, C., Nègre-Salvayre, A., Parini, A., and Vindis, C. (2012) Serotonin 5-HT2A receptor-mediated hypertrophy is negatively regulated by caveolin-3 in cardiomyoblasts and neonatal cardiomyocytes. *J. Mol. Cell. Cardiol.* **52,** 502–510
21. Niwa, N., Yasui, K., Opthof, T., Takemura, H., Shimizu, A., Horiba, M., Lee, J. K., Honjo, H., Kamiya, K., and Kodama, I. (2004) $Ca_v3.2$ subunit underlies the functional T-type Ca^{2+} channel in murine hearts during the embryonic period. *Am. J. Physiol. Heart Circ. Physiol.* **286,** H2257–H2263
22. Yasui, K., Niwa, N., Takemura, H., Opthof, T., Muto, T., Horiba, M., Shimizu, A., Lee, J. K., Honjo, H., Kamiya, K., and Kodama, I. (2005) Pathophysiological significance of T-type Ca^{2+} channels: expression of T-type Ca^{2+} channels in fetal and diseased heart. *J. Pharmacol. Sci.* **99,** 205–210
23. Nuss, H. B., and Houser, S. R. (1993) T-type Ca^{2+} current is expressed in hypertrophied adult feline left ventricular myocytes. *Circ. Res.* **73,** 777–782
24. Ferron, L., Capuano, V., Ruchon, Y., Deroubaix, E., Coulombe, A., and Renaud, J. F. (2003) Angiotensin II signaling pathways mediate expression of cardiac T-type calcium channels. *Circ. Res.* **93,** 1241–1248
25. Sen, L., and Smith, T. W. (1994) T-type Ca^{2+} channels are abnormal in genetically determined cardiomyopathic hamster hearts. *Circ. Res.* **75,** 149–155
26. Huang, B., Qin, D., Deng, L., Boutjdir, M., and El-Sherif, N. (2000) Reexpression of T-type Ca^{2+} channel gene and current in post-infarction remodeled rat left ventricle. *Cardiovasc. Res.* **46,** 442–449
27. Chiang, C. S., Huang, C. H., Chieng, H., Chang, Y. T., Chang, D., Chen, J. J., Chen, Y. C., Chen, Y. H., Shin, H. S., Campbell, K. P., and Chen, C. C. (2009) The Ca(v) 3.2 T-type Ca^{2+} channel is required for pressure overload-induced cardiac hypertrophy in mice. *Circ. Res.* **104,** 522–530
28. Head, B. P., Patel, H. H., Roth, D. M., Lai, N. C., Niesman, I. R., Farquhar, M. G., and Insel, P. A. (2005) G-protein-coupled receptor signaling components localize in both sarcolemmal and intracellular caveolin-3-associated microdomains in adult cardiac myocytes. *J. Biol. Chem.* **280,** 31036–31044
29. Liu, Y., Dillon, A. R., Tillson, M., Makarewich, C., Nguyen, V., Dell'Italia, L., Sabri, A. K., Rizzo, V., and Tsai, E. J. (2013) Volume overload induces differential spatiotemporal regulation of myocardial soluble guanylyl cyclase in eccentric hypertrophy and heart failure. *J. Mol. Cell. Cardiol.* **60,** 72–83
30. Tsai, E. J., Liu, Y., Koitabashi, N., Bedja, D., Danner, T., Jasmin, J. F., Lisanti, M. P., Friebe, A., Takimoto, E., and Kass, D. A. (2012) Pressure-overload-induced subcellular relocalization/oxidation of soluble guanylyl cyclase in the heart modulates enzyme stimulation. *Circ. Res.* **110,** 295–303
31. Pluteanu, F., and Cribbs, L. L. (2009) T-type calcium channels are regulated by hypoxia/reoxygenation in ventricular myocytes. *Am. J. Physiol. Heart Circ. Physiol.* **297,** H1304–H1313
32. Wang, F., Gao, H., Kubo, H., Fan, X., Zhang, H., Berretta, R., Chen, X., Sharp, T., Starosta, T., Makarewich, C., Li, Y., Molkentin, J. D., and Houser, S. R. (2013) T-type Ca^{2+} channels regulate the exit of cardiac myocytes from the cell cycle after birth. *J. Mol. Cell. Cardiol.* **62,** 122–130
33. Zheng, M., Wang, Y., Kang, L., Shimaoka, T., Marni, F., and Ono, K. (2010) Intracellular Ca^{2+}- and PKC-dependent upregulation of T-type Ca^{2+} channels in LPC-stimulated cardiomyocytes. *J. Mol. Cell. Cardiol.* **48,** 131–139
34. Park, J. Y., Kang, H. W., Moon, H. J., Huh, S. U., Jeong, S. W., Soldatov, N. M., and Lee, J. H. (2006) Activation of protein kinase C augments T-type Ca^{2+} channel activity without changing channel surface density. *J. Physiol.* **577,** 513–523
35. Braz, J. C., Gregory, K., Pathak, A., Zhao, W., Sahin, B., Klevitsky, R., Kimball, T. F., Lorenz, J. N., Nairn, A. C., Liggett, S. B., Bodi, I., Wang, S., Schwartz, A., Lakatta, E. G., DePaoli-Roach, A. A., *et al.* (2004) PKC-α regulates cardiac contractility and propensity toward heart failure. *Nat. Med.* **10,** 248–254
36. Bowling, N., Walsh, R. A., Song, G., Estridge, T., Sandusky, G. E., Fouts, R. L., Mintze, K., Pickard, T., Roden, R., Bristow, M. R., Sabbah, H. N., Mizrahi, J. L., Gromo, G., King, G. L., and Vlahos, C. J. (1999) Increased protein kinase C activity and expression of Ca^{2+}-sensitive isoforms in the failing human heart. *Circulation* **99,** 384–391
37. Bkaily, G., Sculptoreanu, A., Wang, S., Nader, M., Hazzouri, K. M., Jacques, D., Regoli, D., D'Orleans-Juste, P., and Avedanian, L. (2005) Angiotensin II-induced increase of T-type Ca^{2+} current and decrease of L-type Ca^{2+} current in heart cells. *Peptides* **26,** 1410–1417
38. Morishima, M., Wang, Y., Akiyoshi, Y., Miyamoto, S., and Ono, K. (2009) Telmisartan, an angiotensin II type 1 receptor antagonist, attenuates T-type Ca^{2+} channel expression in neonatal rat cardiomyocytes. *Eur. J. Pharmacol.* **609,** 105–112
39. Rinne, A., Kapur, N., Molkentin, J. D., Pogwizd, S. M., Bers, D. M., Banach, K., and Blatter, L. A. (2010) Isoform- and tissue-specific regulation of the Ca^{2+}-sensitive transcription factor NFAT in cardiac myocytes and heart failure. *Am. J. Physiol. Heart Circ. Physiol.* **298,** H2001–H2009
40. Wilkins, B. J., De Windt, L. J., Bueno, O. F., Braz, J. C., Glascock, B. J., Kimball, T. F., and Molkentin, J. D. (2002) Targeted disruption of NFATc3, but not NFATc4, reveals an intrinsic defect in calcineurin-mediated cardiac hypertrophic growth. *Mol. Cell. Biol.* **22,** 7603–7613
41. Nattel, S., Maguy, A., Le Bouter, S., and Yeh, Y. H. (2007) Arrhythmogenic ion-channel remodeling in the heart: heart failure, myocardial infarction, and atrial fibrillation. *Physiol. Rev.* **87,** 425–456
42. Martínez, M. L., Heredia, M. P., and Delgado, C. (1999) Expression of T-type Ca^{2+} channels in ventricular cells from hypertrophied rat hearts. *J. Mol. Cell. Cardiol.* **31,** 1617–1625
43. Wang, Y., Tandan, S., Cheng, J., Yang, C., Nguyen, L., Sugianto, J., Johnstone, J. L., Sun, Y., and Hill, J. A. (2008) Ca^{2+}/calmodulin-dependent protein kinase II-dependent remodeling of Ca^{2+} current in pressure overload heart failure. *J. Biol. Chem.* **283,** 25524–25532
44. David, L. S., Garcia, E., Cain, S. M., Thau, E., Tyson, J. R., and Snutch, T. P. (2010) Splice-variant changes of the Ca(V)3.2 T-type calcium channel mediate voltage-dependent facilitation and associate with cardiac hypertrophy and development. *Channels* **4,** 375–389
45. Nakayama, H., Bodi, I., Correll, R. N., Chen, X., Lorenz, J., Houser, S. R., Robbins, J., Schwartz, A., and Molkentin, J. D. (2009) α1G-dependent T-type Ca^{2+} current antagonizes cardiac hypertrophy through a NOS3-dependent mechanism in mice. *J. Clin. Invest.* **119,** 3787–3796
46. Huang, C. H., Chen, Y. C., and Chen, C. C. (2013) Physical interaction between calcineurin and $Ca_v3.2$ T-type Ca^{2+} channel modulates their functions. *FEBS Lett.* **587,** 1723–1730
47. Kinoshita, H., Kuwahara, K., Takano, M., Arai, Y., Kuwabara, Y., Yasuno, S., Nakagawa, Y., Nakanishi, M., Harada, M., Fujiwara, M., Murakami, M., Ueshima, K., and Nakao, K. (2009) T-type Ca^{2+} channel blockade prevents sudden death in mice with heart failure. *Circulation* **120,** 743–752
48. Yamamoto, E., Kataoka, K., Dong, Y. F., Nakamura, T., Fukuda, M., Nako, H., Ogawa, H., and Kim-Mitsuyama, S. (2010) Benidipine, a dihydropyridine L-type/T-type calcium channel blocker, affords additive benefits for prevention of cardiorenal injury in hypertensive rats. *J. Hypertens.* **28,** 1321–1329
49. Bers, D. M., and Despa, S. (2006) Cardiac myocytes Ca^{2+} and Na^+ regulation in normal and failing hearts. *J. Pharmacol. Sci.* **100,** 315–322
50. Wang, Y., Tandan, S., and Hill, J. A. (2014) Calcineurin-dependent ion channel regulation in heart. *Trends Cardiovasc. Med.* **24,** 14–22
51. Nakayama, H., Chen, X., Baines, C. P., Klevitsky, R., Zhang, X., Zhang, H., Jaleel, N., Chua, B. H., Hewett, T. E., Robbins, J., Houser, S. R., and Molkentin, J. D. (2007) Ca^{2+}- and mitochondrial-dependent cardiomyocyte necrosis as a primary mediator of heart failure. *J. Clin. Invest.* **117,** 2431–2444
52. Chen, X., Nakayama, H., Zhang, X., Ai, X., Harris, D. M., Tang, M., Zhang, H., Szeto, C., Stockbower, K., Berretta, R. M., Eckhart, A. D., Koch, W. J., Molkentin, J. D., and Houser, S. R. (2011) Calcium influx through Cav1.2 is a proximal signal for pathological cardiomyocyte hypertrophy. *J. Mol. Cell. Cardiol.* **50,** 460–470
53. Makarewich, C. A., Correll, R. N., Gao, H., Zhang, H., Yang, B., Ber-

retta, R. M., Rizzo, V., Molkentin, J. D., and Houser, S. R. (2012) A caveolae-targeted L-type Ca^{2+} channel antagonist inhibits hypertrophic signaling without reducing cardiac contractility. *Circ. Res.* **110,** 669–674

54. Gao, H., Wang, F., Wang, W., Makarewich, C. A., Zhang, H., Kubo, H., Berretta, R. M., Barr, L. A., Molkentin, J. D., and Houser, S. R. (2012) Ca^{2+} influx through L-type Ca^{2+} channels and transient receptor potential channels activates pathological hypertrophy signaling. *J. Mol. Cell. Cardiol.* **53,** 657–667
55. Wu, X., Eder, P., Chang, B., and Molkentin, J. D. (2010) TRPC channels are necessary mediators of pathologic cardiac hypertrophy. *Proc. Natl. Acad. Sci. U.S.A.* **107,** 7000–7005